

Title: The Antitumor Activities of Anti-CD47 Antibodies Require Fc-Fc γ R interactions

Authors:

Juan C. Osorio^{1,2}, Patrick Smith¹, David A. Knorr^{1,2}, Jeffrey V. Ravetch^{1*}

Affiliations

¹Laboratory of Molecular Genetics and Immunology, Rockefeller University, New York, NY, 10065, USA

²Department of Medicine, Memorial Sloan Kettering Cancer Center, New York, NY, 10065, USA

Correspondence: Jeffrey Ravetch ravetch@rockefeller.edu

Summary

While anti-CD47 antibodies hold promise for cancer immunotherapy, early phase clinical trials have shown limited signs of clinical benefit, suggesting that blockade of CD47 alone may not be sufficient for effective tumor control. Here, we investigate the contributions of the Fc domain of anti-CD47 antibodies required for optimal in vivo antitumor activity across multiple species-matched models, providing new insights into the mechanisms underlying the efficacy of this emerging class of therapeutic antibodies. Using a novel mouse model humanized for CD47, SIRP α and Fc γ Rs, we demonstrate that local administration of an Fc-engineered anti-CD47 antibody with enhanced binding to activating Fc γ Rs modulates myeloid and T-cell subsets in the tumor microenvironment, resulting in improved long-term systemic antitumor immunity and minimal on-target off-tumor toxicity. Our results highlight the importance of Fc optimization in the development of effective anti-CD47 therapies and provide a novel approach for enhancing the antitumor activity of this promising immunotherapy.

Highlights

- Engagement of activating Fc γ Rs augments the in vivo antitumor activity of CD47 blocking antibodies
- Humanized mice for CD47, SIRP α and Fc γ Rs allow assessment of hFc γ Rs contribution to the activity of anti-hCD47 Abs
- Fc-optimized anti-hCD47 ab promotes systemic antitumor immunity with abscopal effect and minimal on-target toxicity

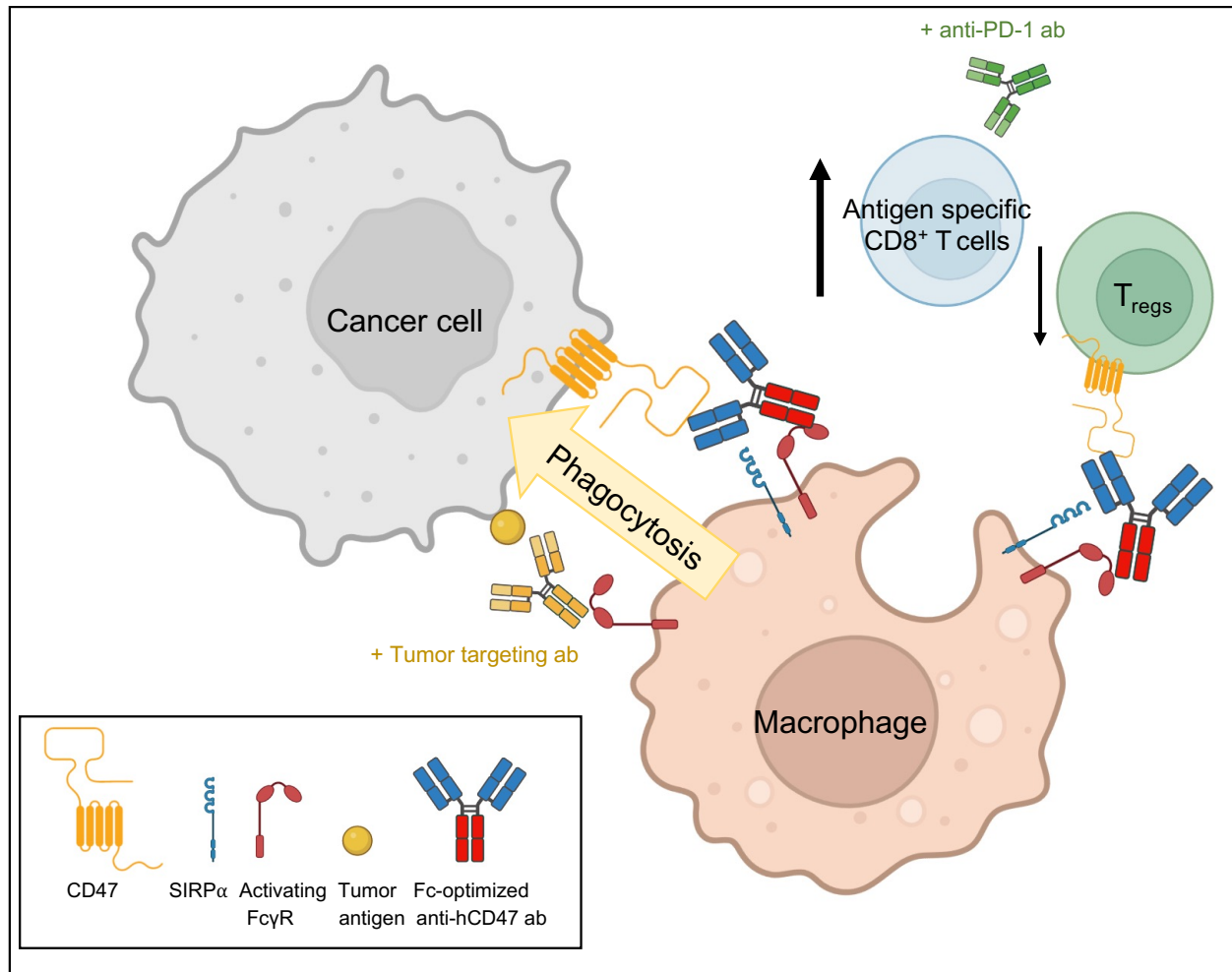
Key Words:

CD47, SIRP α , Fc receptor, antibody engineering, phagocytosis, macrophage, cancer immunotherapy, innate immunity

Abbreviations:

Antibody (ab), bone marrow derived macrophages (BMDM), days (d), extracellular domain (ECD), Fc gamma receptor (Fc γ R), human (h), immunoreceptor tyrosine-based activation motifs (ITAMs), intraperitoneal (IP), intratumoral (IT), knock in (KI), mouse (m), red blood cells (RBC), standard error mean (SEM), subcutaneous, (sq.), tumor microenvironment (TME), wild type (WT).

Graphical Abstract



Graphic design made with Biorender

Introduction

Antibodies (Abs) blocking inhibitory immune checkpoints expressed primarily on adaptive immune cells lead to profound and durable clinical responses in a wide range of malignancies (Ribas and Wolchok, 2018). However, the benefit of these therapies is limited only to a subset of patients. As a result, there is a growing interest in identifying additional checkpoints for cancer immunotherapy including those expressed on innate immune cells. The CD47/SIRP α axis has emerged as an essential checkpoint for cancer immunosurveillance by functioning as a “don’t eat me” signal that suppresses innate immune responses. CD47 is a cell surface receptor expressed on healthy cells and often overexpressed on cancer cells (Willingham et al., 2012), which protects them from phagocytosis by interacting with SIRP α , an inhibitory immunoreceptor expressed on myeloid cells including macrophages, neutrophils and subsets of dendritic cells (Adams et al., 1998). In several preclinical studies, therapeutic antibodies that block the interaction between CD47 and SIRP α promote effective antitumor responses by enabling elimination of both hematologic and solid tumor cells by phagocytes (Chao et al., 2010; Jaiswal et al., 2009; Majeti et al., 2009; Weiskopf et al., 2016; Willingham et al., 2012), enhancing cross-presentation of CD8⁺ T cells by antigen presenting cells, and triggering adaptive immune responses (Liu et al., 2016; Liu et al., 2015b). These encouraging results led the development of several antibodies and fusion proteins blocking CD47, which are now being investigated in over 50 clinical trials across multiple tumor types (Jalil et al., 2020; Uger and Johnson, 2020).

Despite these advances, anti-CD47 antibodies have demonstrated limited clinical benefit when administered as monotherapy (Bouwstra et al., 2022), highlighting the need to better understand the mechanisms behind the efficacy of these therapies. To this end, a critical question that remains to be answered is whether the antitumor activity of these antibodies relies solely on blocking the CD47/SIRP α interaction by the fragment antigen-binding (Fab) domain, or whether interactions between the fragment crystallizable (Fc) and Fc gamma receptors (Fc γ Rs) also contribute to their antitumor activity (Zhao et al., 2012a; Zhao et al., 2012b). Fc γ Rs are functionally classified as activating (Fc γ RI, Fc γ RIIA, Fc γ RIIIA in humans; Fc γ RI, Fc γ RIII, Fc γ RIV in mouse) or inhibitory (Fc γ RIIB in both human and mouse), and are expressed on a variety of cells (Nimmerjahn and Ravetch, 2008). The effector responses mediated by different IgG subclasses are dependent on their differential affinities for activating or

inhibitory Fc γ Rs. As a result, Fc γ R signaling through the Fc portion of IgG antibodies can induce activation of phagocytic and cytotoxic cells, and has been found essential for the therapeutic activity of antibodies targeting tumor antigens (Bevaart et al., 2006; Clynes et al., 2000; DiLillo and Ravetch, 2015), and most recently on antibodies blocking or agonizing immune checkpoints (Dahan et al., 2016; Dahan et al., 2015). Optimization of these interactions have led the development of second-generation antitumor immunotherapies to further enhance their therapeutic potential (Bournazos et al., 2017; Cohen Saban et al., 2023; Garris et al., 2021; Knorr et al., 2018; Liu et al., 2020).

Currently, there is no consensus on the ideal Fc format that will maximize the therapeutic index of Ab targeting CD47. This is evident by the variety of IgG subclasses used to design these therapies for clinical trials (Jalil et al., 2020; Uger and Johnson, 2020). Results from early-phase clinical trials indicate that antibodies with weak or null engagement to Fc γ Rs (hIgG4, hIgG2 or inert Fc region) were relatively tolerable, but did not show clinical benefit when administered as monotherapy (Burris et al., 2021; Sikic et al., 2019; Zeidan et al., 2022). Of note, they only demonstrated benefit in combination with other antitumor antibodies that engage Fc γ Rs such as Rituximab (Abrisqueta et al., 2019; Advani et al., 2018). In contrast to these results, antibodies with competent binding to Fc γ Rs (hIgG1 Fc format) showed the highest levels of therapeutic activity as monotherapy (Ansell et al., 2021; Horwitz et al., 2021; Querfeld et al., 2018); however, low concentrations of the drug were administered due to transient depletion normal CD47-expressing cells such as red blood cells (RBC) and platelets, suggesting that the Fc could also mediate some of the on-target off-tumor toxicity. Overall, these results suggests that simple blockade of the CD47-SIRP α interaction may not be sufficient to induce significant antitumor immunity and that concomitant pro-phagocytic signals, such as engagement of Fc γ Rs may be also necessary. Optimizing the capacity of CD47 blocking antibodies to engage appropriate Fc γ R pathways is expected to promote activation of effector cells in the tumor microenvironment (TME), resulting in significant improvement in their in vivo antitumor activity.

Most preclinical investigations on the therapeutic activity of anti-CD47 antibodies used xenograft (Edris et al., 2012; Weiskopf et al., 2016; Xu et al., 2015) or immune-compromised (Chao et al., 2010; Jaiswal et al., 2009;

Majeti et al., 2009) mouse models. These are limited by substantial interspecies differences between mouse (m) and human (h) CD47-SIRP α as well as Fc-Fc γ R interactions (Kwong et al., 2014; Nimmerjahn and Ravetch, 2008; Subramanian et al., 2006), providing a potential explanation as to why they have failed to correlate with efficacy and toxicity observed in patients. In this study, we provide new insights into the mechanisms behind the therapeutic activity of antibodies targeting CD47 by elucidating the effector functions engaged by Fc-Fc γ R interactions in several immune competent, species-matched tumor models, including a novel mouse model humanized for CD47, SIRP α and Fc γ Rs, which overcomes the limitations of prior studies. In this platform, we evaluate whether Fc γ R singling can be exploited to further augment the antitumor immunity of these therapies and allow us to identify an Fc-optimized antibody targeting human CD47 for effective in vivo antitumor activity.

Results

Engagement of activating Fc γ Rs contributes to in vivo antitumor activity of anti-mCD47 antibodies

To determine the contribution of Fc-Fc γ R interactions to the in vivo activity of antibodies targeting the CD47-SIRP α axis, we modified the Fc domain of the anti-mCD47 antibody (ab) clone MIAP301 to generate antibodies with varying affinity to mFc γ Rs: 1) mIgG2a Fc, binding preferentially to activating mFc γ Rs I and IV, 2) mIgG1 Fc, binding preferentially to the inhibitory mFc γ RIIB, and 3) mIgG1-D265A Fc, which lacks binding to any mFc γ Rs (**Figure S1A**) (Nimmerjahn and Ravetch, 2005). Alterations to the Fc domain of MIAP301 did not alter the binding specificity of the variable regions to mCD47 (**Figure S1C**), nor its in vivo half-life (Dahan et al., 2015) which allows comparisons into the contributions of differential Fc γ R engagement to the activity of CD47 blocking antibodies. We compared the in vivo antitumor activity of these different Fc subclasses of MIAP301 in wild type B6 (WT) mice bearing subcutaneous (sq.) MC38 colorectal adenocarcinomas, a tumor type expressing high levels of CD47 (**Figure S1B**). We found the mIgG2a Fc variant of MIAP301 led to the most significant reduction in tumor burden when compared to the control or other Fc variants (**Figure 1A and S2A**). Of note, this therapeutic effect was attenuated for the mIgG1-D265A Fc variant and in mice lacking all activating Fc γ Rs (FcR- γ chain^{-/-}) (Takai et al., 1994) (**Figure 1A and S2B**). The mIgG2a Fc variant of MIAP301 also demonstrated the most significant decrease in the number of lung metastases in a second tumor model using B16 melanoma cells (**Figure 1B and S2C**).

Currently, there are several clinical trials investigating anti-CD47 antibodies in combination with therapies blocking tumor antigens of immune checkpoints (Maute et al., 2022). We thus compared the anti-tumor activity of the different Fc variants of MIAP301 in combination with a tumor targeting ab against gp75 (Clone TA99, mlgG2a ab) (Clynes et al., 1998) or with an ab blocking the immune checkpoint PD-1 (Clone RMP1-14, mlgG1 D265A ab). To assess these combinations, we used a sq. B16 melanoma model in which none of our MIAP301 Fc variants worked as monotherapy (**Figure 1C and S2D**). The combination of anti-gp75 ab with the MIAP301-mlgG2a ab led to significant reduction in tumor burden when compared to anti-gp75 ab alone or the other combinations (**Figure 1D and S2E**). Similarly, combination of the anti-PD-1 ab with MIAP301-mlgG2a ab significantly decreased tumor burden when compared to PD-1 blockade alone or the other combinations (**Figure 1E and S2F**). The enhanced activity of the mlgG2a ab compared to the other Fc subclasses alone or in combination with tumor targeting antibodies or immune checkpoint blockade indicates that engagement of activating Fc γ Rs by CD47 antibodies contributes to its optimal in vivo anti-tumor activity.

Engagement of activating Fc γ Rs during treatment with anti-CD47 antibodies correlates with increased number of tumor-infiltrating macrophages and enhanced phagocytic activity.

To evaluate the factors that promote the enhanced activity of the mlgG2a Fc subclass of MIAP301, we compared the effect of the three Fc variants on myeloid cells in the TME. Treatment with the MIAP301-mlgG2a ab correlates with a significant increase in the percentage of CD45⁺ leukocytes (**Figure S3A**), mainly attributed to a significant increase in CD11b⁺F4/80⁺ macrophages and CD11b⁺Ly6C⁺ monocytes, but not neutrophils or dendritic cells (**Figure 2A and S3D-E**). These findings suggested that these two populations could mediate the effector response during treatment with this Fc variant. To test this hypothesis, we selectively depleted tumor infiltrating macrophages or CCR2⁺ monocytes using clodronate or an anti-CCR2 ab (mlgG2a), respectively (**Figure S3F-H**). Depletion with clodronate – but not with anti-CCR2 ab – abrogated the activity of the MIAP301-mlgG2a ab (**Figure 2B-C**), indicating that macrophages are required effector cells for the increased therapeutic activity of MIAP301-mlgG2a. Since CD47 constitutes a well-known antiphagocytic signal on macrophages, we assessed the effect of the different anti-mCD47 Fc subclasses in macrophage activity by performing in vitro phagocytosis assays of MC38 and B16 cancer cells using bone marrow derived macrophages (BMDM). The MIAP301-mlgG2a ab led to significantly more phagocytosis of both cancer cell lines when compared to control or the other Fc

subclasses (**Figure 2D and S4A**). These effects were also seen when other murine cancer cells lines were used as targets (**Figure S4B**). Altogether, these results indicate that engagement of activating Fc γ Rs by CD47 antibodies increases the number of tumor-infiltrating macrophages and enhances their tumor phagocytic activity.

Engagement of activating Fc γ Rs during treatment with anti-CD47 antibodies modulates subsets of T cells and promotes long term antitumor immunity

CD47 blockade promotes adaptive immune responses by increasing cross-presentation of tumor antigens (Liu et al., 2015b; Tseng et al., 2013) and by inducing type 1 immune responses through direct ligation of CD47 expressed on T cells (Bouguermouh et al., 2008). We first analyzed the patterns of CD47 expression on CD8⁺, CD4⁺FOXP3⁻, and CD4⁺FOXP3⁺ (Regulatory T cells or T_{regs}) T cells in the TME. We found that all three T cell subsets expressed CD47, however T_{regs} exhibited a significantly higher expression when compared to CD4⁺FOXP3⁻ or CD8⁺ T cells (**Figure 3A**). This differential expression of CD47 supports the possibility that the anti-tumor effect observed after treatment with an Fc-enhanced anti-CD47 ab results from both enhanced phagocytosis and depletion of T_{regs} in the TME. To test this hypothesis, we assessed the effect of the three subclasses of MIAP301 on T_{regs} in the TME of MC38 tumors. Treatment with the MIAP301-mIgG2a ab led to a significant decrease in the percentage of T_{regs} when compared to control tumors (**Figure 3B**), suggesting that treatment with the MIAP301-mIgG2a ab is associated with an Fc-mediated decrease in the frequencies of immunosuppressive CD47^{high} expressing T_{regs}.

Since T_{regs} can restrain effective adaptive antitumor activity (Shan et al., 2022), we investigated whether decreased levels of T_{regs} correlate with a higher number of CD4⁺FOXP3⁻ or CD8⁺ T cells. No significant changes were seen in the percentages of these two populations, however, there was a significant increase in the number of antigen-specific T cells (**Figure 3C and S3B-C**). Furthermore, depletion of CD8⁺ T cells abrogated the antitumor activity of the MIAP301-mIgG2a ab, indicating that CD8⁺ T cells are required for its optimal therapeutic activity (**Figure 3D**). To determine whether tumor-specific T cell responses induced by the MIAP301-mIgG2a ab resulted in long term immune memory, WT mice in which MIAP301-mIgG2a ab led to a complete antitumor response were subsequently rechallenged with a 5-fold higher dose of MC38 tumor cells 90 days following initial tumor challenge in the absence of additional therapy (**Figure 3E**). Mice previously treated with the MIAP301-

mIgG2a ab completely rejected the tumor rechallenge when compared to naïve mice (**Figure 3E**). Overall, these findings indicate that treatment with a mIgG2a anti-CD47 ab facilitates long term CD8⁺ tumor-specific antitumor immunity.

Generation of CD47/SIRP α humanized knock-in mice to assess antibodies targeting human CD47 in vivo

Having established the contribution of mFc γ R engagement in an immune competent murine system, we examined whether our findings were applicable for antibodies targeting human CD47 (hCD47). For this purpose, we developed a humanized mouse strain in which the human extracellular domains (ECD) of CD47 and SIRP α replaced their respective murine counterparts using CRISPR/Cas9 gene-editing (hCD47/hSIRP α knock in (KI) mice) (**Figure S5A**). We assessed the expression pattern of hCD47 and hSIRP α in these mice and found that, similar to the pattern seen on human cells, hCD47 is ubiquitously expressed on peripheral blood red blood cells (RBC), platelets, CD3⁺ and CD11b⁺ cells. In contrast, SIRP α was expressed primarily on CD11b⁺ cells but not in other cells (**Figure 4A**). Peripheral blood levels of RBC, platelets and other leukocytes were similar than those found WT mice (**Figure S5B**). Furthermore, the hCD47 and hSIRP α expressed on these humanized mice were capable of binding their human counterparts (**Figure S5C**). In an analogous CRISPR/Cas9 gene-editing strategy, we generated MC38 and B16 cancer cell lines in which their mouse ECD of CD47 was replaced by the hCD47 ECD (MC38-hCD47 KI, B16-hCD47 KI, respectively) (**Figure S5D-E**). These cell lines can be engrafted in the hCD47/hSIRP α KI mouse system and represent a unique system to test anti-human antibodies.

To test the therapeutic activity of antibodies against hCD47, we used the 5F9 clone (Magrolimab), which is currently being investigated in several clinical trials (Advani et al., 2018). We first generated chimeric antibodies containing human Fab and the three Fc subclasses with varying affinities to mFc γ Rs: 5F9-mIgG2a, 5F9-mIgG1, and 5F9-mIgG1-D265A ab (**Figure S1A and S1D**). Using hCD47/hSIRP α KI mice, we compared the therapeutic activity of the three Fc variants of 5F9 in the MC38 hCD47KI sq. model and the B16 hCD47KI lung metastases model. Similar to the mIgG2a MIAP301 Fc variant, we found the 5F9-mIgG2a ab led to the most significant reduction in tumor burden in both tumor models when compared to control or other Fc variants (**Figure 4B-4C**). Furthermore, the 5F9-mIgG2a ab led to the most significant amount of in vitro phagocytosis of both cancer cells

when compared to control or the other Fc subclasses (**Figure S4C-D**). These effects were also seen under different in vitro macrophage polarization states (**Figure S4E**). Altogether, these results validate our prior findings in the immune competent murine backgrounds and further support the role of activating Fc γ R_s in modulating the in vivo activity of human CD47 antibodies.

Effective in vivo antitumor activity requires both blockade of the CD47/SIRP α axis and engagement of activating Fc γ R signaling

Using our humanized system for CD47 antibodies, we investigated whether engagement of activating Fc γ R_s is sufficient, or whether concomitant blockade of the CD47/SIRP α signal is also required to achieve optimal in vivo therapeutic activity. To address this question, we compared the in vivo antitumor activity of two antibodies targeting hCD47: The 5F9 ab clone which blocks the interaction between CD47 and SIRP α , and the 2D3 ab clone which binds to CD47 but does not block its interaction with SIRP α (Tseng et al., 2013) (**Figure 4D**). Both antibodies were generated as mIgG2a Fc subclass to retain engagement of activating Fc γ R_s, which allowed us to investigate the contribution of the Fab domains to the antitumor activity. We confirmed that both 5F9-mIgG2 and 2D3-mIgG2a bind to hCD47 (**Figure S1E**), but only 5F9-mIgG2a can block the interaction with hSIRP α (**Figure S1F**). Furthermore, we found that similar to the 5F9-mIgG2a ab, the 2D3-mIgG2a ab is capable of inducing in vitro ADCP of cancer cells, indicating its capacity to bind Fc γ R_s (**Figure S4F**). We compared the therapeutic activity of the two antibodies in the B16 hCD47 KI lung metastases model and found that only the 5F9-mIgG2a ab led to significantly decreased tumor burden when compared to the 2D3-mIgG2a ab or control (**Figure 4E**). These results suggest that in order to achieve significant antitumor activity, anti-CD47 antibodies require both mechanisms of activity: blockade of the CD47/SIRP α (antiphagocytic) signal by the Fab domain, and engagement of the activating Fc γ R_s (pro-phagocytic) signal by the Fc domain.

Mice humanized for CD47, SIRP α and Fc γ R are a reliable platform for the evaluation of toxicity and therapeutic activity of fully human anti-CD47 antibodies

After demonstrating the biological rationale for engaging activating Fc γ R_s in both murine and human chimeric anti-CD47 antibodies, we investigated the therapeutic potential of fully humanized anti-CD47 antibodies relevant

for clinical translation. Currently, most anti-hCD47 antibodies translated into patients have been studied in xenograft, immunocompromised or purely murine backgrounds (Edris et al., 2012; Liu et al., 2015b; Majeti et al., 2009; Weiskopf et al., 2016). Unfortunately, these models do not fully recapitulate with the on-target off-tumor toxicity as well as therapeutic activity observed in patients receiving these therapies as monotherapy (Sikic et al., 2019; Zeidan et al., 2022). To overcome this limitation, we crossed our hCD47/hSIRP α KI mice with a mouse humanized for Fc γ Rs, in which all mouse Fc γ R genes have been deleted and all human Fc γ Rs are expressed as transgenes (Smith et al., 2012) (**Figure 6A**). We confirmed that our hCD47/hSIRP α /hFc γ R mice maintain the human cell-type specific expression profile of Fc γ Rs found in the humanized mice for Fc γ Rs (**Figure S6**).

First, we hypothesized that the humanized hCD47/hSIRP α /hFc γ R mice could recapitulate the toxicity observed with CD47 blocking antibodies in the clinical setting, in particular anemia and thrombocytopenia (Oldenburg et al., 2000). To test this hypothesis, we compared the human CD47 blocking antibody 5F9-hIgG4 used in several clinical trials (Advani et al., 2018), with the Fc-optimized variant 5F9-GAALIE. These two antibodies have identical Fab regions, but differ in their Fc: the 5F9-hIgG4 ab is a “weak” engager of Fc γ Rs; in contrast, the 5F9-GAALIE is a human IgG1 Fc format containing three point mutations that enhances binding for all the activating Fc γ Rs and reduced binding to the inhibitory Fc γ R, thus optimizing the A/I ratio (Weitzenfeld et al., 2019) (**Figure 6B**). Systemic administration of these two human antibodies in WT mice did not lead to significant changes in peripheral RBCs or platelets in WT mice (**Figure 6C**). In contrast, increasing dosing concentration of both 5F9-hIgG4 and 5F9-GAALIE antibodies led to anemia and thrombocytopenia in hCD47/hSIRP α /hFc γ R mice. Of note, these effects were transient (lowest values by day 4 to 8) and most of them recovered by day 11. While the 5F9-G4 ab started to decrease the number of RBC and platelets at a high systemic dose (10 mg/Kg) (**Figure 6D**), the 5F9-GAALIE antibody led to anemia and thrombocytopenia at the lowest systemic dose administered (2.5 mg/Kg), with significantly more anemia, thrombocytopenia, and mortality in mice treated a higher dose (5 mg/Kg and 10 mg/Kg) (**Figure 6E**). These findings indicate that engagement of activating Fc γ Rs during CD47 ab blockade also mediates off-tumor on-target toxicity of these therapies, and that the hCD47/hSIRP α /hFc γ R mice provide a unique and reliable platform for the study of clinically relevant Fc-optimized anti-CD47/SIRP α .

antibodies in vivo by recapitulating important parameters of biological activity and toxicity observed in the clinical setting.

Fc-optimized anti-CD47 antibodies promote superior antitumor activity

To evaluate the in vitro activity of the two different Fc formats of hCD47 blocking antibodies, we assessed phagocytosis of B16 hCD47 KI or human cancer cells by macrophages generated from species matched mononuclear cells. The GAALIE 5F9 ab led to significantly more phagocytosis of cancer cells when compared to the hIgG4 format or control (**Figure S4F-S4I**). Given the increased Fc-mediated toxicity observed with systemic administration of the 5F9-GAALIE ab, we next assessed whether direct (intratumoral, IT) delivery of the lowest dose (2.5 mg/kg) of anti-hCD47 antibodies to the tumor site could help control tumor growth while providing an optimal safety profile. Intratumoral administration of the 5F9-GAALIE ab led to a significant reduction in tumor burden when compared to the 5F9-IgG4 ab or control in the MC38 hCD47 KI tumor model (**Figure 6A**). Simultaneously, we evaluated whether this approach could also help control distant (non-injected) tumor growth by inducing an abscopal effect. For this purpose, we used a bilateral flank MC38 hCD47 KI tumor model which allows monitoring of tumors at both treated and untreated sites. We found that the 5F9-GAALIE ab led to significant control of distant tumor growth when compared to control, ultimately leading to complete responses in 5 out of 8 mice (**Figure 6B-C**). Of note, this local dose delivery system also resulted in significantly less toxicity (**Figure 6D**). To investigate the effects of the 5F9-GAALIE ab in a more aggressive tumor model that is traditionally resistant to single agent immune-based therapies (e.g., anti-PD-1), we used the B16 hCD47 KI sq. model (Dahan et al., 2015; Wei et al., 2017). We compared the antitumor activity of the two Fc-formats for anti-CD47 ab and found the 5F9-GAALIE ab led to a significant decrease in tumor burden as monotherapy when compared to 5F9-hIgG4 or control (**Figure 6E**). Furthermore, combination therapy with intratumoral 5F9-GAALIE ab and systemic PD-1 blockade elicited significant improved control of tumor growth when compared to PD-1 blockade administered as monotherapy or control (**Figure 6F**). These results indicate that intratumoral dosing of Fc-optimized anti-hCD47 ab promotes effective antitumor activity, leads to abscopal immunity in distant tumor lesions and synergizes with PD-1 blockade while limiting on-target off-tumor toxicity.

Discussion

The Fc region of antibodies blocking CD47 has been postulated as a potential modulator of their therapeutic activity (Bouwstra et al., 2022; Maute et al., 2022; Zhao et al., 2012b). However, efforts to address this question have been limited to suboptimal preclinical studies, limiting their translational relevance for human therapeutics. In this study, we overcome these limitations by elucidating the in vivo contributions of the Fc region of anti-CD47 antibodies using a novel syngeneic immunocompetent murine model that accurately reflects the affinities and cellular expression of human CD47-SIRP α and IgG-Fc γ Rs axes. As a proof of concept, we use multiple species matched systems to demonstrate that anti-CD47 antibodies displayed enhanced in vivo antitumor activity only when the antibody Fc was optimized to engage activating Fc γ Rs. This effect depends on both macrophages and antigen specific T cells and leads to long-lived systemic immunity. Using this unique platform, we show enhanced in vivo antitumor activity, abscopal antitumor effect and minimal on-target toxicity induced by local administration of the fully human Fc-optimized anti-CD47 ab 5F9-GAALIE as monotherapy or in combination with PD-1 blockade. These data support the importance of Fc optimization in the development of effective anti-CD47 therapies and provide a reliable platform to optimize the therapeutic activity of this promising immunotherapy.

Our studies demonstrate that anti-CD47 antibodies require two mechanisms of action for optimal in vivo activity: 1) Fab-mediated CD47/SIRP α -blocking signal; and 2) Fc-mediated engagement of activating – but not inhibitory – Fc γ Rs. This dual mechanism of action has been considered a critical factor for the activity of other immunomodulatory antibodies. This is the case of antibodies blocking CTLA-4, CCR8, OX-40, 401BB or PD-L1, in which engagement of activating Fc γ Rs seems to augment their therapeutic activity (Arce Vargas et al., 2018; Buchan et al., 2018; Bulliard et al., 2014; Cohen Saban et al., 2023; Knorr et al., 2023; Simpson et al., 2013). In contrast, selective engagement of the inhibitory Fc γ RIIB enhances the activity of agonistic antibodies targeting CD40 (Li and Ravetch, 2011; White et al., 2011). In certain cases, engagement of Fc γ Rs could also compromise the activity of these therapies, which is the case of anti-PD-1 antibodies (Dahan et al., 2015). Furthermore, we observed that optimization of the Fc region of the fully humanized anti-CD47 antibody to selectively engage activating Fc γ Rs significantly augmented the therapeutic activity of these agents in a system that closely recapitulate both human CD47-SIRP α and IgG-Fc γ R signaling. This is important, given the extensive differences

on the pattern of cellular expression and distribution between the mouse and human Fc γ Rs of macrophages and other immune cells in the TME(Bournazos, 2019). These differences further underscores the advantage of using fully humanized Fc-Fc γ R systems to better estimate the activity of these therapies in humans(Bournazos et al., 2014). Altogether, we propose the clinical development and evaluation of second-generation CD47 blocking antibodies with enhanced Fc effector function, which could improve their therapeutic activity and overcome some of the limited clinical benefit observed in early-phase clinical trials.

The improved in vivo activity of anti-CD47 antibodies Fc-enhanced for activating Fc γ Rs is characterized by modulation of several immune cell populations in the TME. Notably, we found a significant increase in macrophages in the TME of treated mice, which likely contribute to their antitumor activity. The central role of macrophages on the in vivo Fc-mediated activity of anti-CD47 antibodies is consistent with our findings and others indicating that Fc-Fc γ R interactions are required to induce significant phagocytosis of cancer cells by human macrophages during treatment with CD47 therapies (Jain et al., 2019; Metayer et al., 2017). This suggest that in order to achieve effective antitumor activity, anti-CD47 antibodies must not only disrupt CD47-SIRP α interactions in macrophages but also opsonize the tumor cells through antibody-dependent cellular phagocytosis (ADCP). Furthermore, downstream interactions between SIRP α and Fc γ R signaling seem to be critical for the effector activity of these cells, with evidence indicating the ratio of activating IgG to inhibitory CD47 blockade dictates macrophage phagocytic activity by increasing phosphorylation of ITAMs on Fc γ Rs(Suter et al., 2021).

In addition to the increased number of macrophages in the TME, we observed a decrease in the frequency of T_{regs}, and an increase in the number of antigen-specific T cells. T_{regs} are a specialized sub-population of T cells that diminish effective antitumor immune responses and are an attractive target for cancer immunotherapy (Togashi et al., 2019). Of note, we observed that T_{regs} express high levels of CD47 when compared to other CD4⁺ or CD8⁺ T cells, a finding that has been observed in CTLA-4⁺ T_{regs} obtained from human tumor samples(Zhang et al., 2021). While reduced differentiation or proliferation of T_{regs} could be induced by “reprogrammed” macrophages after Fc-mediated phagocytosis of cancer cells(Tseng et al., 2013), our data suggest that Fc-optimized anti-CD47 antibodies promote T_{reg} depletion likely contributing to a less immunosuppressive TME. Nevertheless, our findings suggest that in addition to modulation of myeloid effector

activity, Fc-optimized anti-CD47 antibodies also promote systemic and long-lasting adaptive immune responses by downregulating immunosuppressive T cell populations and enabling effective tumor antigen-specific cytotoxic T cell responses. The alterations in the frequency of these T cell populations in the TME may also explain the abscopal effects observed after local administration of the CD47 antibody 5F9-GAALIE, as well the long-term immune memory in the tumor rechallenge experiments.

On-target toxicity resulting from phagocytosis of normal CD47-expressing cells (i.e., RBCs and platelets) during treatment with anti-CD47 antibodies remains a concern for the clinical implementation of these therapies. The lack of cross-reactivity between most human CD47 blocking antibodies and their murine counterparts has been a major limitation of murine models. (Huang et al., 2017). Furthermore, these systems may overestimate the efficacy of these therapies as they failed to account for the large CD47 antigenic sink from normal cells. Nonhuman primates are a better system to assess toxicity (Liu et al., 2015a; Meng et al., 2019; Puro et al., 2020), however their use for simultaneous assessment of antitumor activity or alternative delivery or dosing systems are limited. Our humanized model overcomes these limitations and provides a system for simultaneous assessment of on-target off-tumor toxicity and antitumor activity. Our results indicate that the Fc region of CD47 antibodies contributes to such toxicities. These results have significant implications on the development of novel CD47 blocking agents that balance the anti-cancer Fc-mediated effects with the potential hazardous off-tumor side effects. To overcome this limitation, we tested intratumoral delivery of the 5F9-GAALIE ab, which maximizes durable control of local and distant tumor growth while minimizing on-target toxicity. Finally, we observed that combination with therapies, such as PD-1 blockade, can further enhance the systemic long-term immunity and is an attractive potential avenue to explore in patients.

The CD47-SIRP α axis is a promising target in cancer immunotherapy with a rapidly developing field in recent years. By elucidating the *in vivo* contributions of Fc γ R signaling in the antitumor activity and toxicity of fully humanized anti-CD47 antibodies, our findings address a critical question in the field that will inform the rational development of Fc-optimized anti-CD47 antibodies.

Methods

Mouse strains

C57BL/6J (WT) (Strain#: 000664) mice were purchased from The Jackson Laboratory. Mice humanized for Fc γ Rs (hFc γ Rs mouse: murine α chain KO, Fc γ RI⁺, Fc γ RIIA^{R131+}, Fc γ RIIB⁺, Fc γ RIIIA^{F158+}, Fc γ RIIIB⁺) were generated and extensively characterized in our laboratory as previously described (Smith et al., 2012). The Fc receptor common γ -chain deficient mice (FcR- γ chain^{-/-}) were generated in our laboratory as previously described (Takai et al., 1994).

Mice humanized for CD47 and SIRP α (hCD47/hSIRP α knock-in) were generated independently on the C57BL/6J background by CRISPR/Cas9-mediated gene-targeting strategy. For each gene, the extracellular domain of mouse CD47 (exon 2) and mouse SIRP α (exon 2) were excised by sgRNAs and replaced with their respective human exon 2 transgene sequences (via synthesized MegaMers, IDT) through non-homologous end joining (NHEJ). To target the mouse *CD47* and *SIRP α* genes, CRISPR sgRNAs (UpCD47C-TTGCATCGTCCGTAATGTGG**AGG**, DnCD47D-ATAGAGCTGAAAAACCGCAC**GGG** and UpSIRP α A-AAATCAGTGTCTGTTGCTGCT**TGG**, UpSIRP α E-GGAACAGAGGTCTATGTACT**CGG** (PAMS in bold) were used to guide the Alt-R™ S.p. HiFi Cas9 Nuclease (IDT) creating double stranded breaks.

To create the humanized CD47 knock-in, the corresponding CRISPR/Cas9 reagents were microinjected into C57BL/6 (Jackson Laboratories) 1-cell stage mouse embryos and then implanted into surrogate CD-1 mice (Charles River Laboratories). Pups born were screened for presence of the targeted allele and analyzed for proper expression. The transgenesis of the humanized SIRP α knock-in utilized a different approach to deliver the CRISPR/Cas9 kit called “improved-Genome editing via Oviduct Nucleic Acids Delivery (i-Gonad) (Ohtsuka et al., 2018). Similarly, pups born from recipient female mice were screened for presence of the Exon 2 knock-in and analyzed for proper expression. Mice humanized for hCD47 and hSIRP α (hCD47/hSIRP α KI) were generated by backcrossing a hCD47 knock-in mouse to a hSIRP α knock-in mouse. Mice humanized for CD47, SIRP α and Fc γ Rs (hCD47/hSIRP α /hFc γ R) were generated by backcrossing a fully hCD47/hSIRP α KI mouse to hFc γ R mice. All mice were bred and housed at Rockefeller University Comparative Bioscience Center under specific pathogen-free conditions. All mice used were 7 to 12-week-old at time of the experiment, with a mix of

male and female mice. All experiments were performed in compliance with institutional guidelines and were approved by the Rockefeller University Institutional Animal Care and Use Committee (IACUC).

Cell lines and Cell culture

Murine MC38 colorectal cancer, B16 melanoma, Lewis Lung carcinoma (LLC) and human Jurkat and Raji lymphoma cells and were obtained from ATCC. HKP1 ($Kras^{G12D}p53^{-/-}$) lung adenocarcinoma cells were characterized and obtained from the laboratory of Dr. Vivek Mittal (Markowitz et al., 2018). All murine cells were maintained in DMEM (Life Technologies) supplemented with 10% fetal bovine serum (Life Technologies), 100 U/mL of penicillin, and 100 μ g/mL of streptomycin (Life Technologies). Jurkat and Raji cells were maintained in RPMI-1640 Medium supplemented with 10% fetal bovine serum (Life Technologies), and 100 U/mL of penicillin, and 100 μ g/mL of streptomycin (Life Technologies). Cells were split twice per week and cell viability was measured using trypan blue staining in the Countess II automated cell counter (Thermo Fisher). MC38 hCD47 KI and B16 hCD47 KI cancer cells were generated through CRISPR/Cas9-mediated gene targeting by replacing the extracellular domain of mouse CD47 (exon 2) by their respective human counterpart through non-homologous end joining. CRISPR sgRNA (U*C*U*GCAUAUAUGAUUAUCUU and A*C*C*UUGCAGAAGUCACUAG) were synthesized and purchased from Synthego. hCD47 (exon 2) HRD was purchased from Integrated DNA technologies (IDT). Cells were subsequently sorted using anti-hCD47 and anti-mCD47 antibodies, to obtain cells that homogeneously expressed only human CD47.

Antibody engineering and expression

The variable heavy and light regions of anti-hCD47 ab clone 5F9 was synthesized (IDT) based on its published sequence (patent US9382320B2). The variable heavy and light regions of the anti-CD47 antibodies MIAP301 (anti-mCD47 ab) and 2D3 (nonblocking anti-hCD47 antibody) were decoded by mass spectrometry analysis (Bioinformatics Solutions, Inc.). The variable region sequences of the parental antibodies were subcloned and inserted into mammalian expression vectors with human IgG1, human IgG4, mouse IgG2, mouse IgG1 heavy chains, or human κ or mouse κ light chains, as previously described (Li and Ravetch, 2011). For the generation of Fc-domain variants of human IgG1 (GAALIE: G236A/A330L/I332E) and mouse IgG1 (D265A), site-directed mutagenesis using specific primers was performed based on the QuikChange site-directed mutagenesis Kit II

(Agilent Technologies) according to the manufacturer's instructions. Mutated plasmid sequences were validated by direct sequencing (Genewiz).

Antibodies were generated by transient cotransfection of Expi293F cells with heavy-chain and light-chain constructs. Expi293F cells were maintained in serum-free Expi293 Expression Medium and transfected using an ExpiFectamine 293 Transfection Kit (all from Thermo Fischer Scientific). Supernatants were collected 7 days after transfection, centrifuged, and filtered (0.22 μ m). Antibodies were purified from clarified supernatants using Protein G Sepharose 4 Fast Flow (GE Healthcare), dialyzed in PBS, and sterile filtered (0.22 μ m) as previously described (Nimmerjahn et al., 2005).

ELISA assays

Binding specificity of antibodies targeting mouse (MIAP301) and human (2D3 and 5F9) monoclonal antibodies were determined by ELISA using recombinant mouse (SinoBiological 57231-MNAH) and human (SinoBiological 12283-HCCH) CD47, respectively. Blocking activity of 5F9-mIgG2a and 2D3-mIgG2a was determined by competitive ELISA using recombinant human SIRP α -hFc (SinoBiological 11612-H02H1). The 96 well ELISA Half Area High Binding plates (Greiner Bio-One, #675061) were coated overnight at 4°C with recombinant CD47 proteins (1 μ g/mL). All sequential steps were performed at room temperature. After washing, the plates were blocked for 1 hour with 1X PBS containing 2% BSA), and were subsequently incubated for 1 hour with serially diluted IgGs (dilutions are indicated in the figures and were prepared in blocking solution). After washing, plates were incubated for 1 hour with horseradish peroxidase conjugated anti-human or anti-mouse IgG (Jackson ImmunoResearch). For competitive ELISAs, after blocking nonspecific sites, plates were incubated for 1 hour with 1 μ g/mL of human SIRP α -hFc in 1XPBS with 1% BSA. After washing, plates were incubated for 1 hour with serially diluted 5F9-mIgG2a or 2D3-mIgG2a in 1X PBS with 1% BSA. After washing, plates were incubated for 1 hour with horseradish peroxidase conjugated anti-human IgG (#109-035-088, Jackson ImmunoResearch). Detection was performed using a one component substrate solution (TMB), and reactions stopped with the addition of 2 M phosphoric acid. Absorbance at 450 nm was immediately recorded using a SpectraMax Plus spectrophotometer (Molecular Devices), and background absorbance from negative control samples was subtracted.

Tumor challenge, antibody treatments, and myeloid cell depletion

MC38 (2×10^6 cell/mouse), MC38-hCD47KI (5×10^6 cell/mouse), B16 (5×10^5 cell/mouse), or B16-hCD47KI (5×10^5 cell/mouse) were inoculated subcutaneously and tumor volumes were measured biweekly with an electronic caliper and reported as volume (mm^3) using the formula $(L1^2 \times L2)/2$, where L1 is the shortest diameter and L2 is the longest diameter. Mice were randomized and treated with systemic or intratumoral injections as indicated in the figures. For the lung metastases model, B16 or B16-hCD47KI (5×10^5 cell/mouse) were inoculated IV into the lateral tail vein in 200 μL PBS. Mice were randomized and received intraperitoneal injections of 20 mg/Kg on days 1, 4, 7, and 11 after inoculation. The lungs were harvested on day 14 and analyzed for the presence of surface metastatic foci using a dissecting microscope.

Macrophage depletion was performed by intratumoral administration of clodronate liposomes (100 μL /mouse; Catalog F70101C-2, Formumax Scientific Inc) or control liposomes on days 4 and 7 after tumor cell inoculation. CCR2⁺ monocyte depletion was performed by systemic administration of anti-CCR2 antibody (Clone MC-21, 100 μg) or isotype control on day 7 after tumor inoculation. CD8⁺ T cell depletion was performed by systemic administration of anti-CD8 antibody (Clone 2.43, 100 μg , BioXcell) or isotype control on day 7 after tumor inoculation.

Tissue processing

Tumors were dissected and cut into small pieces and transferred to gentleMACS C tubes (Miltenyi Biotec) containing enzyme mix for tough tumors (Catalog 130-096-730m Miltenyi Biotec) in Dulbecco's modified Eagle's medium (DMEM) (Biological Industries). Tumors were then dissociated using the gentleMACS OctoDissociator with Heaters (gentleMACS Program 37Cm_TDK_2, Miltenyi Biotec). Cell suspensions were then dispersed through a 70- μm nylon cell strainer and washed with PBS.

Hematological analysis

50-100 μL blood samples were obtained from the retro-orbital sinus of mice under isoflurane anesthesia. Blood was placed in BD Microtainer tubes coated with ethylene diaminetetraacetic acid (K2-EDTA) and peripheral blood cell (RBC and platelets) counts were measured by Element HT5 hematology analyzer (Heska).

Flow cytometry

Surface expression of mouse or human CD47 on murine tumor cell lines was assessed using MIAP301-PE (Biolegend) and CC2C6-APC (Biolegend) or 5F9-APC (generated in our lab) antibodies, respectively. Tumor cells (5×10^5) were incubated with 0.5 μ g antibody. Baseline staining was obtained using isotype-matched antibodies as controls.

Cell suspensions from tumors were isolated as described above, then stained for viability using the Aqua Amine fixable live dead dye (Thermo Fisher Scientific) in PBS at room temperature using standard protocols, then cells were washed once, and resuspended in FACS buffer (PBS with 0.5% BSA and 2 mM EDTA) with Fc blocked using human TrueStain FcX (Biolegend) and incubated in the dark for 10 min at room temperature. For cell surface staining, cells were stained in 100 μ L of FACS buffer and incubated for 30 minutes at 4C. For antigen-specific T cells CD8⁺ T cells, surface staining with an MC38 tumor antigen-derived peptide KSPWFTTL-H-2K^b tetramer was performed (KSPWFTTL-APC, MBL)(Lee et al., 2020). For intracellular Foxp3 staining, an additional step was performed using the Foxp3/Transcription Factor Staining Bugger Set (cat. no. 00-5523, eBioscienceTM) and FOXP3-BV421 or FOXP3-PE (Clone 150D, Biolegend) according to manufacture instructions. Cell populations were defined by the following markers: macrophages: CD45⁺, NK1.1⁻, Ly6C⁻, Ly6G⁻, CD11b⁺, F4/80⁺; monocytes: CD45⁺, NK1.1⁻, CD11b⁺, Ly6C⁺, Ly6G⁻, F4/80⁻; neutrophils: CD45⁺, NK1.1⁻, CD11b⁺, Ly6G⁺, Ly6C^{low/-}, F4/80⁻; DCs: CD45⁺, NK1.1⁻, F4/80⁻, CD11c⁺, MHC-II⁺; NK cells: CD45⁺, NK1.1⁺; CD8 T cells: CD45⁺, CD3⁺, CD8⁺, CD4⁻; Tetramer⁺ CD8 T cells: CD45⁺, CD3⁺, CD8⁺, KSPWFTTL-H-2Kb⁺, CD4⁻; CD4 T cells: CD45⁺, CD3⁺, CD4⁺, CD8⁻, Foxp3⁻; T_{regs}: CD45⁺, CD3⁺, CD4⁺, CD8⁻, Foxp3⁺. Samples were analyzed using an Attune NxT flow cytometer (Thermo Fisher) and data was analyzed using FCS Express 7 Research.

In vitro antibody-dependent macrophage phagocytosis (ADCP)

Bone marrow cells from the tibia and femurs of B6 mice were flushed using a syringe into DMEM (Life Technologies) supplemented with 10% fetal bovine serum (Life Technologies), 100 U/mL of penicillin, and 100 μ g/mL of streptomycin (Life Technologies). Cells were centrifuged followed by RBC lysis (Biolegend) for 5 min, quenched with complete media, and filtered through a 70- μ M cell strainer. Cells were centrifugated and resuspended in media containing 10 ng/mL macrophage-colony stimulating factor (M-CSF) (Peprotech), and

plated on 10-cm untreated petri dishes per mouse in 15 mL of media and cultured for 7 days without replenishing or changing media to derive BMDMs. For polarization to M1 macrophages, cells were washed with complete media on day 8 and were cultured in 15 mL of new media with 10 ng/mL of M-CSF, 90 ng/mL of IFN- γ (Peprotech) and 10 ng/mL of LPS for 24 hours. For polarization to M2 macrophages, cells were washed with complete media on day 8 and were cultured in 15 mL of new media with 10 ng/mL of M-CSF, 90 ng/mL of IL-4 (Peprotech) and 400 ng/mL of IL-13 (Peprotech) for 24 hours.

To quantify ADCP, tumor cells were stained with carboxyfluorescein succinimidyl ester (CFSE), washed with serum-free DMEM, and plated at a density of 150,000 cells per well in 150 μ L serum-free DMEM in a 96-well ultra-low attachment round-bottom plate (Cat. no. 7007; Costar) on ice. Tumor cells were opsonized by addition of 10 μ L/mL of the various Fc variants of CD47 antibodies or control for 30 min on ice. Macrophages (BMDMs or human macrophages derived from PBMCs) were harvested by cell scraping, pelleted, washed in serum-free DMEM, and added to opsonized tumor cells at a density of 50,000 cells per well in 50 μ L of media for a final assay volume of 200 μ L and an effector-to-tumor cell ratio of 1:3. Cells were incubated at 37 °C for 2 h, pelleted, washed FACS buffer and stained with a 1:100 dilution of anti-mF4/80 or anti-m/hCD11b antibody (Biolegend) FACS buffer for 30 min at 4 °C. Cells were pelleted, washed with TrypLE and FACS buffer, and analyzed by flow cytometry using an Attune NxT flow cytometer (Thermo Fisher) and data was analyzed using FCS Express 7 Research. Phagocytosis was determined by the percentage of CFSE⁺ cells within the macrophage cell gate (CD11b⁺/F480⁺). Results are shown as fold change when compared to the level of phagocytosis in cells treated with control.

Statistics

Data was analyzed using Prism GraphPad software. One-way ANOVA with Tukey's multiple comparison test was used to compare 3 or more groups. Unpaired 2-tailed *t* test was used when two groups were compared. All data, unless otherwise indicated, are plotted as mean \pm standard deviation (SD). For statistical test, *P* values of ≤ 0.05 were considered to be statistically significant, indicated as **P* ≤ 0.05 , ***P* ≤ 0.01 , ****P* ≤ 0.001 , and *****P* ≤ 0.0001 , not significant values are denoted as n.s. Lines associated with asterisks indicate groups compared for significance.

Acknowledgements: We thank Maria L. Baez, Alessandra E. Marino, and Carlo M. Sevilla for their excellent technical assistance. We also thank all the members of the J.V.R. Laboratory of Molecular Genetics and Immunology for helping discussions and sharing experiment materials, in particular Stylianos Bournazos for reviewing the manuscript and providing valuable feedback. M. Mack (University Hospital Regensburg) for providing us the anti-CCR2 antibody (clone MC-21)

Author contributions:

Conceptualization, J.C.O, D.A.K., and J.V.R.; **Methodology**, J.C.O, and D.A.K.; **Validation**, J.C.O, P.A.S., **Formal Analysis**, J.C.O, P.A.S.; **Writing**, J.C.O, D.A.K., and J.V.R.; **Resources**, J.C.O, and J.V.R.; **Supervision**, J.C.O, D.A.K., and J.V.R.

Funding: Research reported in this publication was supported by the National Cancer Institute (NCI) of the National Institutes of Health (NIH) under Award Number K08CA266740 to J.C.O; R01CA244327 and R35CA196620 to J.V.R. The content is solely the responsibility of the authors and does not necessarily represent the official views of the NIH. The project described was also supported in part by the grant # UL1TR001866 from the National Center for Advancing Translational Sciences (NCATS, National Institutes of Health (NIH) Clinical and Translational Science Award (CTSA) program, the Memorial Sloan Kettering Cancer Center (MSK) Gerstner Physician Scholars Program, and the NIH/NCI Cancer Center Support Grant P30 CA008748.

Declaration of interest: The authors declare no financial conflicts of interest relevant to this work.

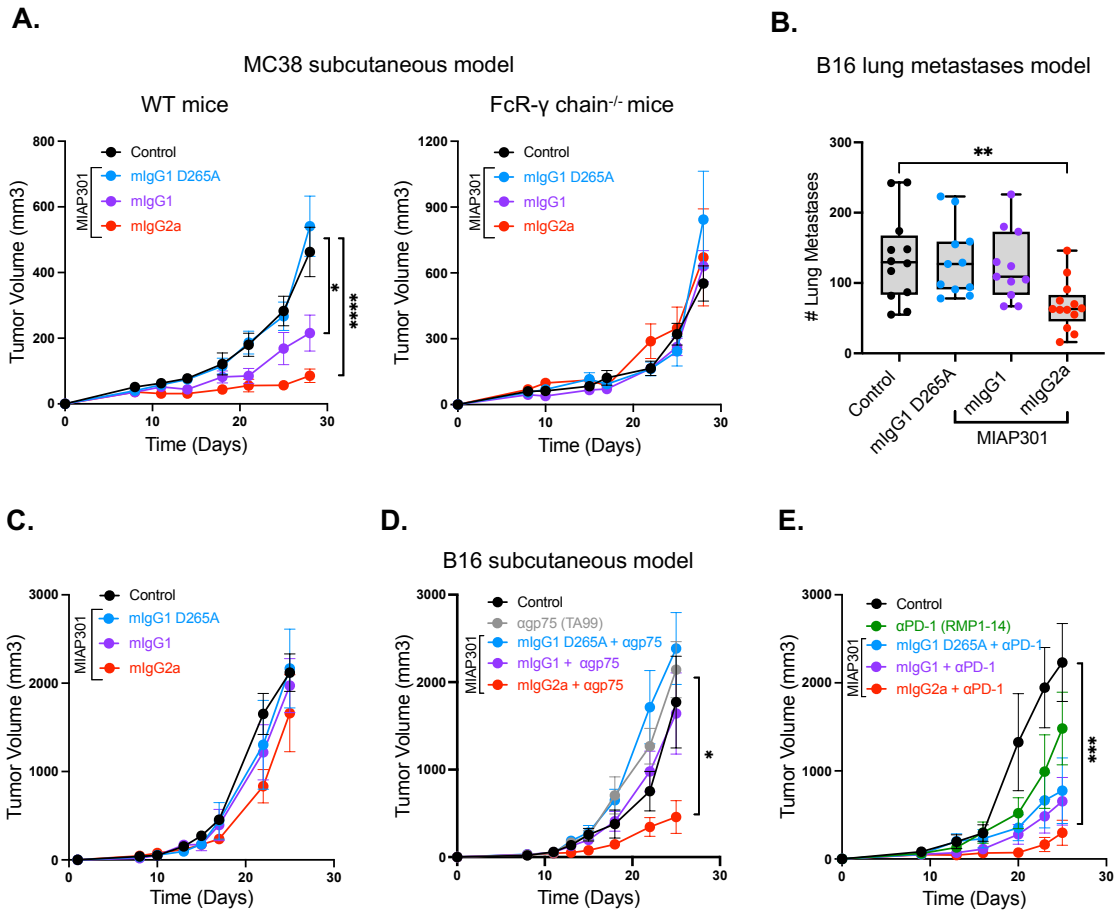


Figure 1. Engagement of activating Fc γ R_s enhances in vivo antitumor activity of antibodies blocking mouse CD47. (A) Average growth \pm SEM of sq. MC38 tumors in WT (right) or FcR- γ chain^{-/-} mice (left), treated with Fc variants of anti-mCD47 ab (MIAP301) or control (50ug IT, d. 8,10,14 and 18). **(B)** Average of lung metastases \pm (Min to Max) of WT mice inoculated IV with B16 tumor cells, treated with anti-mCD47 ab Fc variants (MIAP301) or control (20 mg/Kg IP, d. 1,4,7 and 11). **(C)** Average growth \pm SEM of sq. B16 tumors in WT mice, treated with MIAP301 Fc variants or control (50ug IT, d. 8,10,14 and 18). **(D)** Average growth \pm SEM of sq. B16 tumors in WT mice, treated with MIAP301 Fc variants or control (50 ug IT, d. 8,10,14 and 18) in combination with anti-gp75 ab (TA99-mIgG2a, 200 ug IP d. 8, 10, 14 and 18). **(E)** Average growth \pm SEM of sq B16 tumors in WT mice, treated with MIAP301 Fc variants or control (50ug IT, d. 8,10,14 and 18) in combination with anti-PD-1 ab (RMP1-14-mIgG1-D265A, 200 ug IP d. 8, 10, 14 and 18).

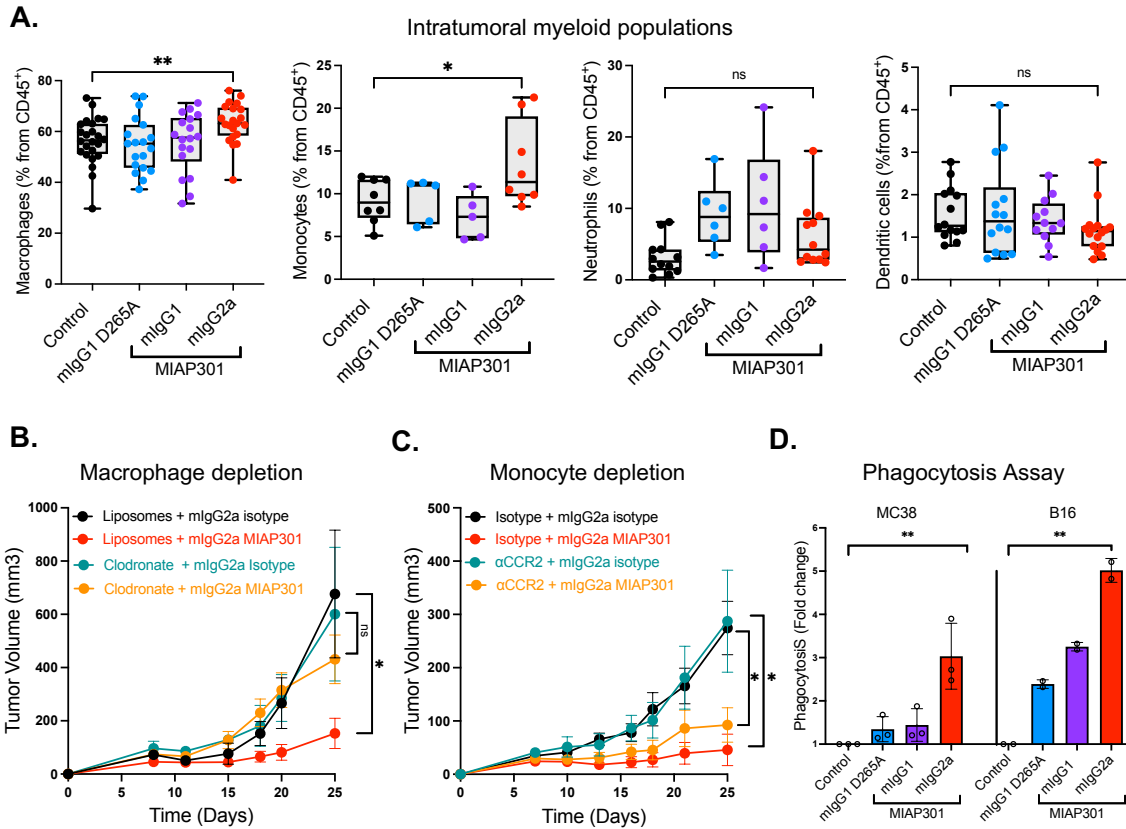


Figure 2. Anti-mCD47 ab Fc-enhanced for activating Fc γ Rs correlates with increased number of tumors infiltrating macrophages and enhanced phagocytic activity. (A) Established MC38 tumors were analyzed by flow cytometry 72 hours after treatment with Fc variants of anti-mCD47 ab (MIAP301). Quantification of intratumoral myeloid cell populations is shown. **(B)** Average growth \pm SEM of sq. MC38 tumors pre-treated with clodronate- or control-liposomes (100 μ L, d.4, 7), then treatment with MIAP301-mlgG2a or isotype control was given (50 μ g IT, d. 8, 10, 14 and 18). **(C)** Average growth \pm SEM of subcutaneous sq. MC38 tumors pre-treated with anti-CCR2 ab (MC-21) or isotype control (100 μ g, d. 7), then treatment with MIAP301- mlgG2a or isotype control was given (50 μ g IT, d. 8, 10, 14 and 18). **(D)** Bone marrow derived macrophages obtained from WT mice were cocultured with CFSE-labeled MC38 or B16 tumor cells in the presence of PBS (Control) or Fc-modified anti-mCD47 ab (MIAP301). Percentage of phagocytosis was determined by the percentage of CFSE⁺ cells within the macrophage cell gate (CD11b⁺F480⁺). Analysis on fold changes compared to control is shown.

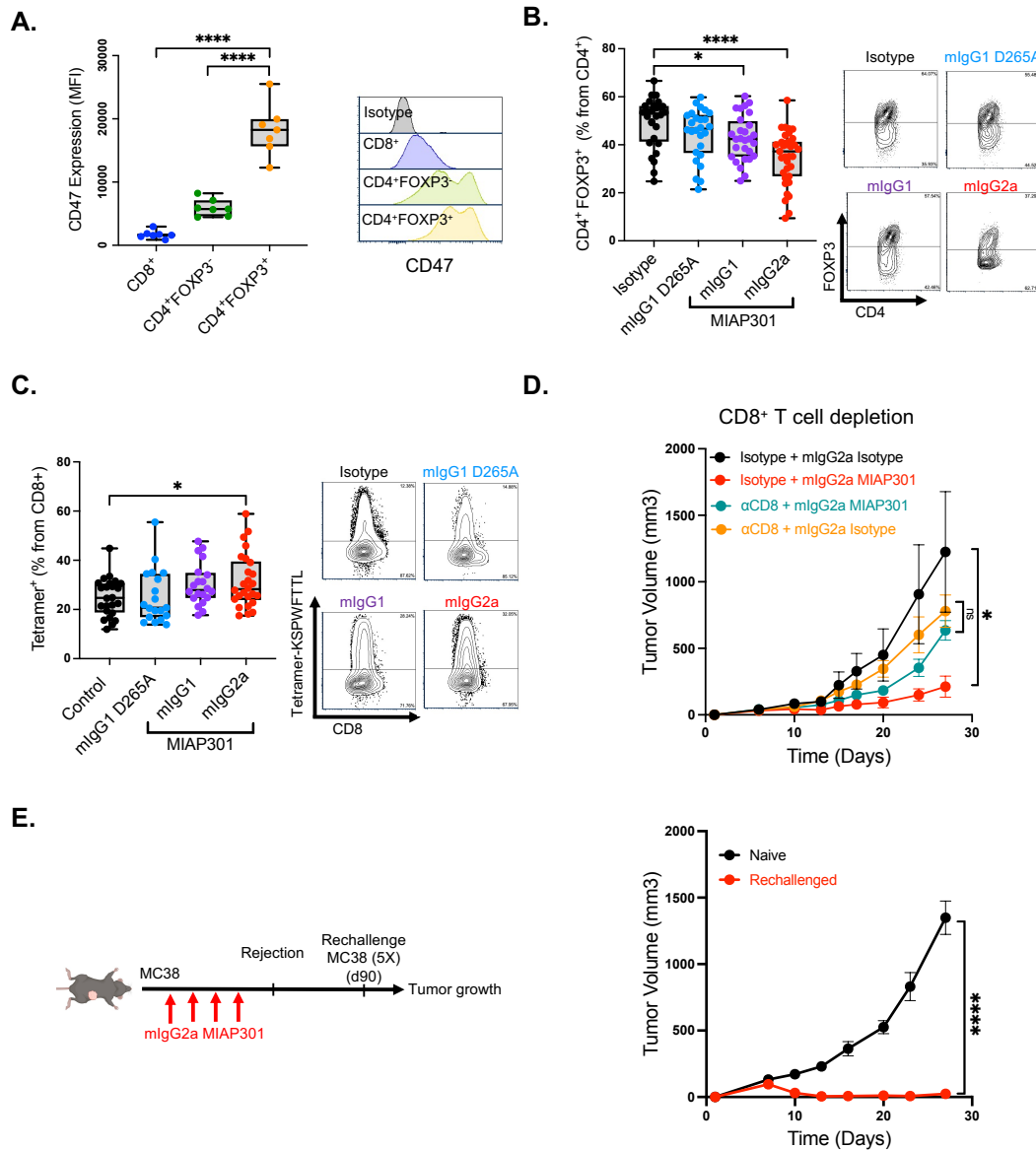


Figure 3. Fc-optimized anti-mCD47 antibodies decreases T_{regs} and promotes infiltration of antigen-specific CD8⁺ T cells. (A) Levels of expression of CD47 on T cell subsets isolated from MC38 tumors, quantification (left) and representative flow cytometry plots (right) are shown. (B) Percentage of CD4⁺FOXP3⁺ T_{regs} of total CD4⁺ T cells, and (C) Percentage of tetramer⁺ (KSPWFTTL) cells of total CD8⁺ T cells from MC38 tumors 72 hours after treatment with Fc variants of anti-mCD47 abs (MIAP301). (D) Average growth \pm SEM of sq. MC38 tumors pre-treated with anti-CD8 ab (2.43) or isotype control (100 ug. d.7, 12, 17), then treatment with MIAP301-mlgG2a or isotype control was given (50 ug IT, d. 8, 10, 14 and 18). (E, left) MC38 tumors were treated with MIAP301-mlg2a (50 ug every 3 days) until rejection was achieved. Then mice were rechallenged with MC38 cells (10 million, d. 90). (E, right) Average growth \pm SEM of sq. MC38 tumors in mice that achieved rejection 90 days before (rechallenged group) or in mice without prior implantation of MC38 tumors (naïve group).

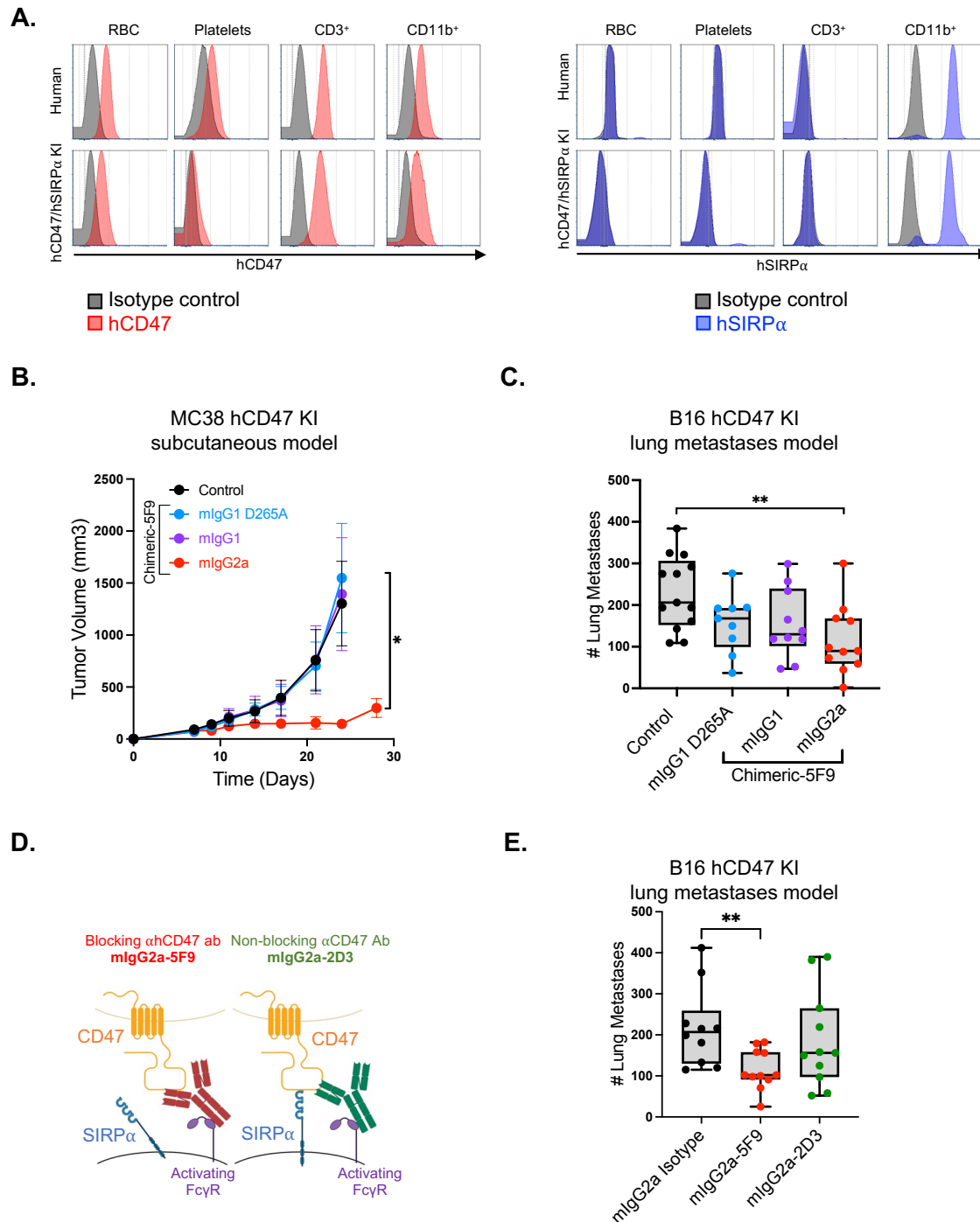


Figure 4. Characterization of hCD47/hSIRP α KI mice and antitumor activity of blocking and non-blocking hCD47 antibodies Fc enhanced for activating Fc γ Rs. (A) Flow cytometry analysis of hCD47 and hSIRP α in red blood cells (RBC), platelets, CD3 $^+$ and CD11b $^+$ leucocytes isolated from peripheral blood of human (top) and hCD47/hSIRP α KI mice (bottom). **(B)** Average growth \pm SEM of sq. MC38 hCD47 KI tumors in hCD47/hSIRP α KI mice, treated with chimeric anti-hCD47 ab Fc variants (chimeric-5F9) or isotype control (50 ug IT, d. 8,10,14 and 18). **(C)** Average of lung metastases \pm SD of hCD47/hSIRP α KI mice inoculated IV with B16 hCD47 KI tumor

cells, treated with chimeric anti-hCD47 ab Fc variants (chimeric-5F9) or isotype control (20 mg/Kg IP, d. 1,4,7 and 11). **(D)** Schematic drawing showing the two ab formats proposed for effective antitumor activity of anti-CD47 antibodies. Left: An ab blocking the interaction between CD47 and SIRP α AND an Fc domain engaging activating Fc γ Rs. Right: A non-blocking anti-CD47 ab AND an Fc domain engaging activating Fc γ Rs. **(E)** Average of lung metastases \pm SD of hCD47/hSIRP α KI mice inoculated IV with B16 hCD47 KI tumor cells, treated with blocking (5F9-mIgG2a) and non-blocking (2D3-mIgG2a) chimeric anti-hCD47 antibodies or isotype control (20 mg/Kg IP, d. 1,4,7 and 11).

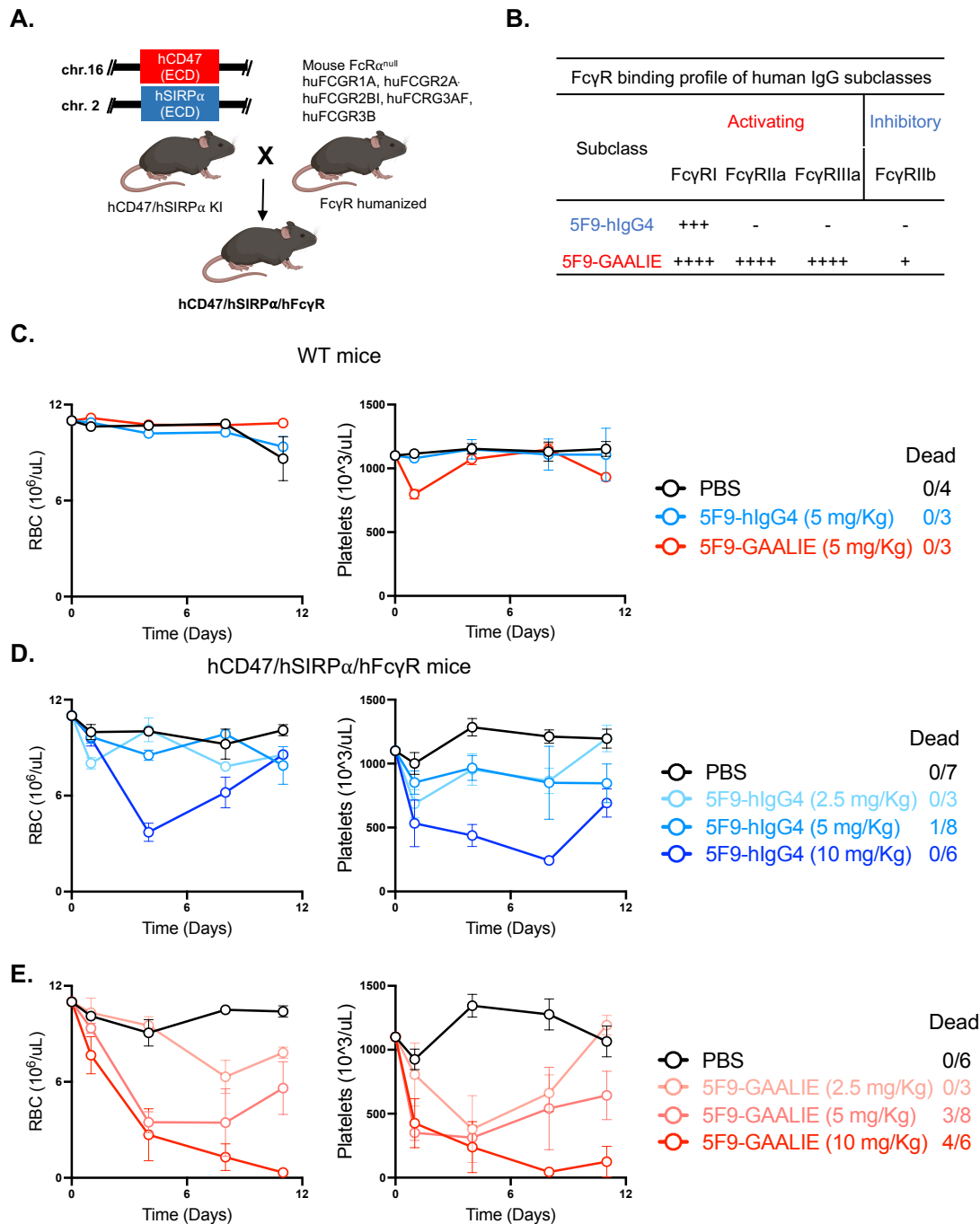


Figure 5. Humanized mouse model for CD47, SIRP α , and Fc γ R recapitulates activity and toxicity profile of fully humanized anti-CD47 antibodies. (A) Schematic drawing showing the generation of the hCD47/hSIRP α /hFc γ R mice **(B)** Binding profiles to hFc γ Rs of Fc variants for anti-hCD47 abs (5F9). **(C)** Peripheral RBC and platelet counts from WT mice after treatment with 5F9-hIgG4 and 5F9-GAALIE (5 mg/Kg d. 0, 4, 8 and 11). **(D)** Peripheral RBC and platelet counts from hCD47/hSIRP α /hFc γ R mice after treatment with increasing doses of 5F9-hIgG4 or **(E)** 5F9-GAALIE ab (2.5, 5, and 10 mg/Kg d. 0, 4, 8 and 11)

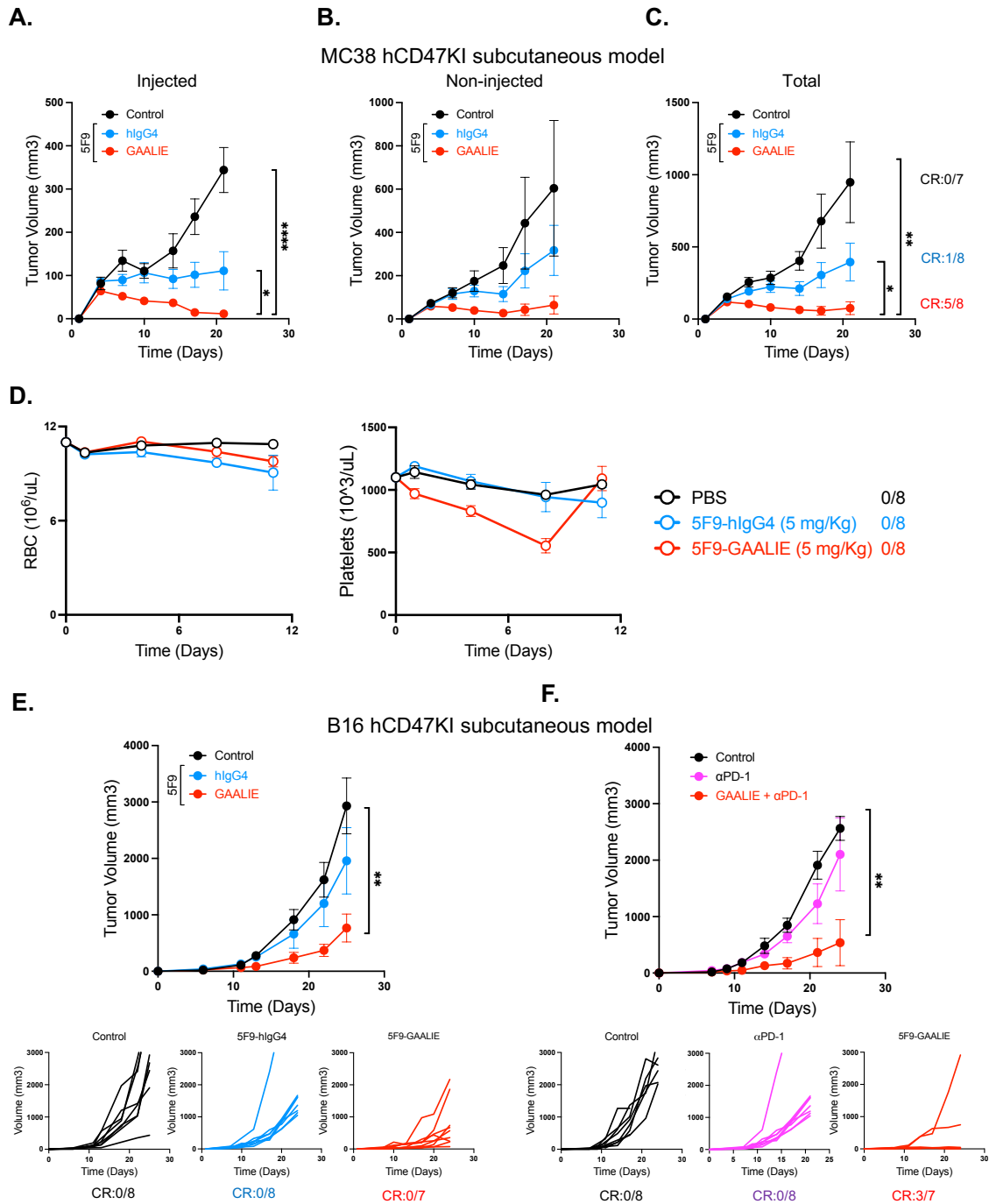


Figure 6. Fc-optimized humanized anti-CD47 Ab promotes effective in vivo antitumor activity

(A) Average growth \pm SEM of injected sq. MC38 hCD47 KI tumors in hCD47/hSIRP α /hFcyR, treated with 5F9-hlgG4, 5F9-GAALIE ab or control (50ug IT, d. 7, 9, and 12). **(B)** Average growth \pm SEM of non-injected contralateral sq. MC38 hCD47 KI tumors in hCD47/hSIRP α /hFcyR mice, treated with treated with 5F9-hlgG4, 5F9-GAALIE ab or control (50ug IT, d. 7, 9, and 12). **(C)** Average growth \pm SEM of total (injected and non-injected) sq. MC38 hCD47 KI tumors in hCD47/hSIRP α /hFcyR, treated with 5F9-hlgG4, 5F9-GAALIE ab or control (50ug IT, d. 7, 9, and 12). **(D)** Serial measurements of peripheral RBC and platelets from

hCD47/hSIRP α /hFc γ R mice after treatment with 5F9-hIgG4 or 5F9-GAALIE (d. 0 indicates the day when treatment was started). **(F)** Average growth \pm SEM of sq. B16 hCD47 KI tumors in hCD47/hSIRP α /hFc γ R, treated with 5F9-hIgG4, 5F9-GAALIE ab or control (50ug IT, d. 8,10,14 and 18). **(G)** Average growth \pm SEM of sq. B16 hCD47 KI tumors in hCD47/hSIRP α /hFc γ R, treated with 5F9-hIgG4, 5F9-GAALIE ab alone (50ug IT, d. 8,10,14 and 18), or in combination with anti-PD1 ab (RMP1-14, 200 ug IP d. 8, 10, 14 and 18), or control.

References

- Abrisqueta, P., Sancho, J. M., Cordoba, R., Persky, D. O., Andreadis, C., Huntington, S. F., Carpio, C., Giles, D. M., Wei, X., Li, Y. F., *et al.* (2019). Anti-CD47 Antibody, CC-90002, in Combination with Rituximab in Subjects with Relapsed and/or Refractory Non-Hodgkin Lymphoma (R/R NHL). *Blood* *134*.
- Adams, S., van der Laan, L. J., Vernon-Wilson, E., Renardel de Lavalette, C., Dopp, E. A., Dijkstra, C. D., Simmons, D. L., and van den Berg, T. K. (1998). Signal-regulatory protein is selectively expressed by myeloid and neuronal cells. *J Immunol* *161*, 1853-1859.
- Advani, R., Flinn, I., Popplewell, L., Forero, A., Bartlett, N. L., Ghosh, N., Kline, J., Roschewski, M., LaCasce, A., Collins, G. P., *et al.* (2018). CD47 Blockade by Hu5F9-G4 and Rituximab in Non-Hodgkin's Lymphoma. *N Engl J Med* *379*, 1711-1721.
- Ansell, S. M., Maris, M. B., Lesokhin, A. M., Chen, R. W., Flinn, I. W., Sawas, A., Minden, M. D., Villa, D., Percival, M. M., Advani, A. S., *et al.* (2021). Phase I Study of the CD47 Blocker TTI-621 in Patients with Relapsed or Refractory Hematologic Malignancies. *Clin Cancer Res* *27*, 2190-2199.
- Arce Vargas, F., Furness, A. J. S., Litchfield, K., Joshi, K., Rosenthal, R., Ghorani, E., Solomon, I., Lesko, M. H., Ruef, N., Roddie, C., *et al.* (2018). Fc Effector Function Contributes to the Activity of Human Anti-CTLA-4 Antibodies. *Cancer Cell* *33*, 649-663 e644.
- Barnes, N., Gavin, A. L., Tan, P. S., Mottram, P., Koentgen, F., and Hogarth, P. M. (2002). FcγRI-deficient mice show multiple alterations to inflammatory and immune responses. *Immunity* *16*, 379-389.
- Bevaart, L., Jansen, M. J., van Vugt, M. J., Verbeek, J. S., van de Winkel, J. G., and Leusen, J. H. (2006). The high-affinity IgG receptor, FcγRI, plays a central role in antibody therapy of experimental melanoma. *Cancer Res* *66*, 1261-1264.
- Bouguermouh, S., Van, V. Q., Martel, J., Gautier, P., Rubio, M., and Sarfati, M. (2008). CD47 expression on T cell is a self-control negative regulator of type 1 immune response. *J Immunol* *180*, 8073-8082.
- Bournazos, S. (2019). IgG Fc Receptors: Evolutionary Considerations. *Curr Top Microbiol Immunol* *423*, 1-11.
- Bournazos, S., DiLillo, D. J., and Ravetch, J. V. (2014). humanized mice to study FcγRI function. *Curr Top Microbiol Immunol* *382*, 237-248.
- Bournazos, S., Wang, T. T., Dahan, R., Maamary, J., and Ravetch, J. V. (2017). Signaling by Antibodies: Recent Progress. *Annual Review of Immunology* *35*, 285-311.
- Bouwstra, R., van Meerten, T., and Bremer, E. (2022). CD47-SIRPα blocking-based immunotherapy: Current and prospective therapeutic strategies. *Clin Transl Med* *12*, e943.
- Buchan, S. L., Dou, L., Remer, M., Booth, S. G., Dunn, S. N., Lai, C., Semmrich, M., Teige, I., Martensson, L., Penfold, C. A., *et al.* (2018). Antibodies to Costimulatory Receptor 4-1BB Enhance Anti-tumor Immunity via T Regulatory Cell Depletion and Promotion of CD8 T Cell Effector Function. *Immunity* *49*, 958-970 e957.
- Bulliard, Y., Jolicoeur, R., Zhang, J., Dranoff, G., Wilson, N. S., and Brogdon, J. L. (2014). OX40 engagement depletes intratumoral Tregs via activating FcγRI, leading to antitumor efficacy. *Immunol Cell Biol* *92*, 475-480.
- Burriss, H. A., Spira, A. I., Taylor, M. H., Yeku, O. O., Liu, J. F., Munster, P. N., Hamilton, E. P., Thomas, J. S., Gatlin, F., Penson, R. T., *et al.* (2021). A first-in-human study of AO-176, a highly differentiated anti-CD47 antibody, in patients with advanced solid tumors. *Journal of Clinical Oncology* *39*.
- Chao, M. P., Alizadeh, A. A., Tang, C., Myklebust, J. H., Varghese, B., Gill, S., Jan, M., Cha, A. C., Chan, C. K., Tan, B. T., *et al.* (2010). Anti-CD47 antibody synergizes with rituximab to promote phagocytosis and eradicate non-Hodgkin lymphoma. *Cell* *142*, 699-713.
- Clynes, R., Takechi, Y., Moroi, Y., Houghton, A., and Ravetch, J. V. (1998). Fc receptors are required in passive and active immunity to melanoma. *Proc Natl Acad Sci U S A* *95*, 652-656.
- Clynes, R. A., Towers, T. L., Presta, L. G., and Ravetch, J. V. (2000). Inhibitory Fc receptors modulate in vivo cytotoxicity against tumor targets. *Nat Med* *6*, 443-446.

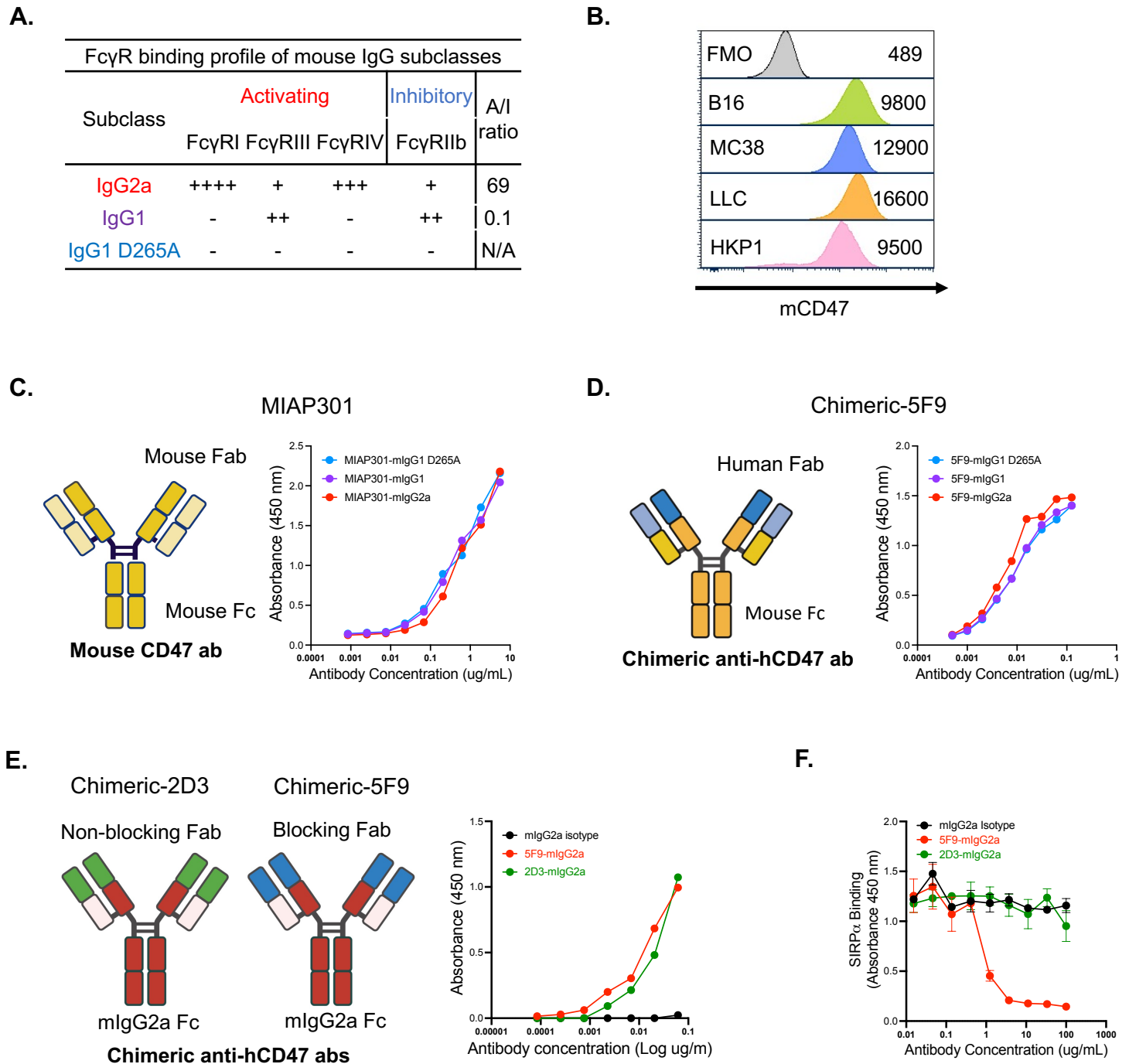
- Cohen Saban, N., Yalin, A., Landsberger, T., Salomon, R., Alva, A., Feferman, T., Amit, I., and Dahan, R. (2023). Fc glycoengineering of a PD-L1 antibody harnesses Fcγ receptors for increased antitumor efficacy. *Sci Immunol* 8, eadd8005.
- Dahan, R., Barnhart, B. C., Li, F., Yamniuk, A. P., Korman, A. J., and Ravetch, J. V. (2016). Therapeutic Activity of Agonistic, Human Anti-CD40 Monoclonal Antibodies Requires Selective FcγR Engagement. *Cancer Cell* 29, 820-831.
- Dahan, R., Segal, E., Engelhardt, J., Selby, M., Korman, A. J., and Ravetch, J. V. (2015). FcγRs Modulate the Anti-tumor Activity of Antibodies Targeting the PD-1/PD-L1 Axis. *Cancer Cell* 28, 543.
- DiLillo, D. J., and Ravetch, J. V. (2015). Fc-Receptor Interactions Regulate Both Cytotoxic and Immunomodulatory Therapeutic Antibody Effector Functions. *Cancer Immunol Res* 3, 704-713.
- Edris, B., Weiskopf, K., Volkmer, A. K., Volkmer, J. P., Willingham, S. B., Contreras-Trujillo, H., Liu, J., Majeti, R., West, R. B., Fletcher, J. A., *et al.* (2012). Antibody therapy targeting the CD47 protein is effective in a model of aggressive metastatic leiomyosarcoma. *Proc Natl Acad Sci U S A* 109, 6656-6661.
- Garris, C. S., Wong, J. L., Ravetch, J. V., and Knorr, D. A. (2021). Dendritic cell targeting with Fc-enhanced CD40 antibody agonists induces durable antitumor immunity in humanized mouse models of bladder cancer. *Sci Transl Med* 13.
- Horwitz, S. M., James, M. F., Maris, M., Lue, J. K., Sawas, A., Okada, C., Feldman, T. A., Sokol, L., Mei, M., Flinn, I. W., *et al.* (2021). Updates from Ongoing, First-in-Human Phase 1 Dose Escalation and Expansion Study of TTI-621, a Novel Biologic Targeting CD47, in Patients with Relapsed or Refractory Hematologic Malignancies. *Blood* 138.
- Huang, Y., Ma, Y., Gao, P., and Yao, Z. (2017). Targeting CD47: the achievements and concerns of current studies on cancer immunotherapy. *J Thorac Dis* 9, E168-E174.
- Jain, S., Van Scoyk, A., Morgan, E. A., Matthews, A., Stevenson, K., Newton, G., Powers, F., Autio, A., Louissaint, A., Pontini, G., *et al.* (2019). Targeted inhibition of CD47-SIRPα requires Fc-FcγR interactions to maximize activity in T-cell lymphomas. *Blood* 134, 1430-1440.
- Jaiswal, S., Jamieson, C. H., Pang, W. W., Park, C. Y., Chao, M. P., Majeti, R., Traver, D., van Rooijen, N., and Weissman, I. L. (2009). CD47 is upregulated on circulating hematopoietic stem cells and leukemia cells to avoid phagocytosis. *Cell* 138, 271-285.
- Jalil, A. R., Andrechak, J. C., and Discher, D. E. (2020). Macrophage checkpoint blockade: results from initial clinical trials, binding analyses, and CD47-SIRPα structure-function. *Antib Ther* 3, 80-94.
- Knorr, D., Leidner, R., Jensen, S., Meng, R., Jones, A., Ballesteros-Merino, C., Bell, R. B., Baez, M., Sprott, D., Bifulco, C., *et al.* (2023). FcγRIIB is a novel immune checkpoint in the tumor microenvironment limiting activity of Treg-targeting antibodies. *bioRxiv*.
- Knorr, D. A., Dahan, R., and Ravetch, J. V. (2018). Toxicity of an Fc-engineered anti-CD40 antibody is abrogated by intratumoral injection and results in durable antitumor immunity. *Proc Natl Acad Sci U S A* 115, 11048-11053.
- Kwong, L. S., Brown, M. H., Barclay, A. N., and Hatherley, D. (2014). Signal-regulatory protein alpha from the NOD mouse binds human CD47 with an exceptionally high affinity-- implications for engraftment of human cells. *Immunology* 143, 61-67.
- Lee, J. C., Mehdizadeh, S., Smith, J., Young, A., Mufazalov, I. A., Mowery, C. T., Daud, A., and Bluestone, J. A. (2020). Regulatory T cell control of systemic immunity and immunotherapy response in liver metastasis. *Sci Immunol* 5.
- Li, F., and Ravetch, J. V. (2011). Inhibitory Fcγ receptor engagement drives adjuvant and anti-tumor activities of agonistic CD40 antibodies. *Science* 333, 1030-1034.
- Liu, J., Wang, L., Zhao, F., Tseng, S., Narayanan, C., Shura, L., Willingham, S., Howard, M., Prohaska, S., Volkmer, J., *et al.* (2015a). Pre-Clinical Development of a Humanized Anti-CD47 Antibody with Anti-Cancer Therapeutic Potential. *PLoS One* 10, e0137345.

- Liu, Q., Wen, W., Tang, L., Qin, C. J., Lin, Y., Zhang, H. L., Wu, H., Ashton, C., Wu, H. P., Ding, J., *et al.* (2016). Inhibition of SIRPalpha in dendritic cells potentiates potent antitumor immunity. *Oncoimmunology* *5*, e1183850.
- Liu, R., Oldham, R. J., Teal, E., Beers, S. A., and Cragg, M. S. (2020). Fc-Engineering for Modulated Effector Functions-Improving Antibodies for Cancer Treatment. *Antibodies (Basel)* *9*.
- Liu, X., Pu, Y., Cron, K., Deng, L., Kline, J., Frazier, W. A., Xu, H., Peng, H., Fu, Y. X., and Xu, M. M. (2015b). CD47 blockade triggers T cell-mediated destruction of immunogenic tumors. *Nat Med* *21*, 1209-1215.
- Majeti, R., Chao, M. P., Alizadeh, A. A., Pang, W. W., Jaiswal, S., Gibbs, K. D., Jr., van Rooijen, N., and Weissman, I. L. (2009). CD47 is an adverse prognostic factor and therapeutic antibody target on human acute myeloid leukemia stem cells. *Cell* *138*, 286-299.
- Markowitz, G. J., Havel, L. S., Crowley, M. J., Ban, Y., Lee, S. B., Thalappillil, J. S., Narula, N., Bhinder, B., Elemento, O., Wong, S. T., *et al.* (2018). Immune reprogramming via PD-1 inhibition enhances early-stage lung cancer survival. *JCI Insight* *3*.
- Maute, R., Xu, J., and Weissman, I. L. (2022). CD47-SIRPalpha-targeted therapeutics: status and prospects. *Immuno-oncol Technol* *13*, 100070.
- Meng, Z., Wang, Z. Y., Guo, B. S., Cao, W., and Shen, H. Q. (2019). TJC4, a Differentiated Anti-CD47 Antibody with Novel Epitope and RBC Sparing Properties. *Blood* *134*.
- Metayer, L. E., Vilalta, A., Burke, G. A. A., and Brown, G. C. (2017). Anti-CD47 antibodies induce phagocytosis of live, malignant B cells by macrophages via the Fc domain, resulting in cell death by phagoptosis. *Oncotarget* *8*, 60892-60903.
- Nimmerjahn, F., Bruhns, P., Horiuchi, K., and Ravetch, J. V. (2005). FcγRIV: a novel FcR with distinct IgG subclass specificity. *Immunity* *23*, 41-51.
- Nimmerjahn, F., Lux, A., Albert, H., Woigk, M., Lehmann, C., Dudziak, D., Smith, P., and Ravetch, J. V. (2010). FcγRIV deletion reveals its central role for IgG2a and IgG2b activity in vivo. *Proc Natl Acad Sci U S A* *107*, 19396-19401.
- Nimmerjahn, F., and Ravetch, J. V. (2005). Divergent immunoglobulin g subclass activity through selective Fc receptor binding. *Science* *310*, 1510-1512.
- Nimmerjahn, F., and Ravetch, J. V. (2008). Fcγ receptors as regulators of immune responses. *Nat Rev Immunol* *8*, 34-47.
- Ohtsuka, M., Sato, M., Miura, H., Takabayashi, S., Matsuyama, M., Koyano, T., Arifin, N., Nakamura, S., Wada, K., and Gurumurthy, C. B. (2018). i-GONAD: a robust method for in situ germline genome engineering using CRISPR nucleases. *Genome Biol* *19*, 25.
- Oldenborg, P. A., Zheleznyak, A., Fang, Y. F., Lagenaur, C. F., Gresham, H. D., and Lindberg, F. P. (2000). Role of CD47 as a marker of self on red blood cells. *Science* *288*, 2051-2054.
- Puro, R. J., Bouchlaka, M. N., Hiebsch, R. R., Capoccia, B. J., Donio, M. J., Manning, P. T., Frazier, W. A., Karr, R. W., and Pereira, D. S. (2020). Development of AO-176, a Next-Generation Humanized Anti-CD47 Antibody with Novel Anticancer Properties and Negligible Red Blood Cell Binding. *Molecular Cancer Therapeutics* *19*, 835-846.
- Querfeld, C., Thompson, J., Taylor, M. H., Pillai, R., Johnson, L. D., Catalano, T., Petrova, P. S., Thompson, T., Uger, R. A., Shou, Y., and Akilov, O. E. (2018). Intralesional Administration of the CD47 Antagonist TTI-621 (SIRPαFc) Induces Responses in Both Injected and Non-Injected Lesions in Patients with Relapsed/Refractory Mycosis Fungoides and Sézary Syndrome: Interim Results of a Multicenter Phase I Trial. *Blood* *132*, 1653-1653.
- Ribas, A., and Wolchok, J. D. (2018). Cancer immunotherapy using checkpoint blockade. *Science* *359*, 1350-1355.
- Shan, F., Somasundaram, A., Bruno, T. C., Workman, C. J., and Vignali, D. A. A. (2022). Therapeutic targeting of regulatory T cells in cancer. *Trends Cancer* *8*, 944-961.

- Sikic, B. I., Lakhani, N., Patnaik, A., Shah, S. A., Chandana, S. R., Rasco, D., Colevas, A. D., O'Rourke, T., Narayanan, S., Papadopoulos, K., *et al.* (2019). First-in-Human, First-in-Class Phase I Trial of the Anti-CD47 Antibody Hu5F9-G4 in Patients With Advanced Cancers. *J Clin Oncol* **37**, 946-953.
- Simpson, T. R., Li, F., Montalvo-Ortiz, W., Sepulveda, M. A., Bergerhoff, K., Arce, F., Roddie, C., Henry, J. Y., Yagita, H., Wolchok, J. D., *et al.* (2013). Fc-dependent depletion of tumor-infiltrating regulatory T cells co-defines the efficacy of anti-CTLA-4 therapy against melanoma. *J Exp Med* **210**, 1695-1710.
- Smith, P., DiLillo, D. J., Bournazos, S., Li, F., and Ravetch, J. V. (2012). Mouse model recapitulating human Fcγ receptor structural and functional diversity. *Proc Natl Acad Sci U S A* **109**, 6181-6186.
- Subramanian, S., Parthasarathy, R., Sen, S., Boder, E. T., and Discher, D. E. (2006). Species- and cell type-specific interactions between CD47 and human SIRPα. *Blood* **107**, 2548-2556.
- Suter, E. C., Schmid, E. M., Harris, A. R., Voets, E., Francica, B., and Fletcher, D. A. (2021). Antibody:CD47 ratio regulates macrophage phagocytosis through competitive receptor phosphorylation. *Cell Rep* **36**, 109587.
- Takai, T., Li, M., Sylvestre, D., Clynes, R., and Ravetch, J. V. (1994). FcR γ chain deletion results in pleiotropic effector cell defects. *Cell* **76**, 519-529.
- Togashi, Y., Shitara, K., and Nishikawa, H. (2019). Regulatory T cells in cancer immunosuppression - implications for anticancer therapy. *Nat Rev Clin Oncol* **16**, 356-371.
- Tseng, D., Volkmer, J. P., Willingham, S. B., Contreras-Trujillo, H., Fathman, J. W., Fernhoff, N. B., Seita, J., Inlay, M. A., Weiskopf, K., Miyanishi, M., and Weissman, I. L. (2013). Anti-CD47 antibody-mediated phagocytosis of cancer by macrophages primes an effective antitumor T-cell response. *Proc Natl Acad Sci U S A* **110**, 11103-11108.
- Uger, R., and Johnson, L. (2020). Blockade of the CD47-SIRPα axis: a promising approach for cancer immunotherapy. *Expert Opin Biol Ther* **20**, 5-8.
- Wei, S. C., Levine, J. H., Cogdill, A. P., Zhao, Y., Anang, N. A. S., Andrews, M. C., Sharma, P., Wang, J., Wargo, J. A., Pe'er, D., and Allison, J. P. (2017). Distinct Cellular Mechanisms Underlie Anti-CTLA-4 and Anti-PD-1 Checkpoint Blockade. *Cell* **170**, 1120-1133 e1117.
- Weiskopf, K., Jahchan, N. S., Schnorr, P. J., Cristea, S., Ring, A. M., Maute, R. L., Volkmer, A. K., Volkmer, J. P., Liu, J., Lim, J. S., *et al.* (2016). CD47-blocking immunotherapies stimulate macrophage-mediated destruction of small-cell lung cancer. *J Clin Invest* **126**, 2610-2620.
- Weitzenfeld, P., Bournazos, S., and Ravetch, J. V. (2019). Antibodies targeting sialyl Lewis A mediate tumor clearance through distinct effector pathways. *J Clin Invest* **129**, 3952-3962.
- White, A. L., Chan, H. T., Roghanian, A., French, R. R., Mockridge, C. I., Tutt, A. L., Dixon, S. V., Ajona, D., Verbeek, J. S., Al-Shamkhani, A., *et al.* (2011). Interaction with FcγRIIb is critical for the agonistic activity of anti-CD40 monoclonal antibody. *J Immunol* **187**, 1754-1763.
- Willingham, S. B., Volkmer, J. P., Gentles, A. J., Sahoo, D., Dalerba, P., Mitra, S. S., Wang, J., Contreras-Trujillo, H., Martin, R., Cohen, J. D., *et al.* (2012). The CD47-signal regulatory protein α (SIRPα) interaction is a therapeutic target for human solid tumors. *Proc Natl Acad Sci U S A* **109**, 6662-6667.
- Xu, J. F., Pan, X. H., Zhang, S. J., Zhao, C., Qiu, B. S., Gu, H. F., Hong, J. F., Cao, L., Chen, Y., Xia, B., *et al.* (2015). CD47 blockade inhibits tumor progression human osteosarcoma in xenograft models. *Oncotarget* **6**, 23662-23670.
- Zeidan, A. M., DeAngelo, D. J., Palmer, J., Seet, C. S., Tallman, M. S., Wei, X., Raymon, H., Sriraman, P., Kopytek, S., Bewersdorf, J. P., *et al.* (2022). Phase 1 study of anti-CD47 monoclonal antibody CC-90002 in patients with relapsed/refractory acute myeloid leukemia and high-risk myelodysplastic syndromes. *Ann Hematol* **101**, 557-569.
- Zhang, A., Ren, Z., Tseng, K. F., Liu, X., Li, H., Lu, C., Cai, Y., Minna, J. D., and Fu, Y. X. (2021). Dual targeting of CTLA-4 and CD47 on T(reg) cells promotes immunity against solid tumors. *Sci Transl Med* **13**.
- Zhao, X. W., Kuijpers, T. W., and van den Berg, T. K. (2012a). Is targeting of CD47-SIRPα enough for treating hematopoietic malignancy? *Blood* **119**, 4333-4334; author reply 4334-4335.

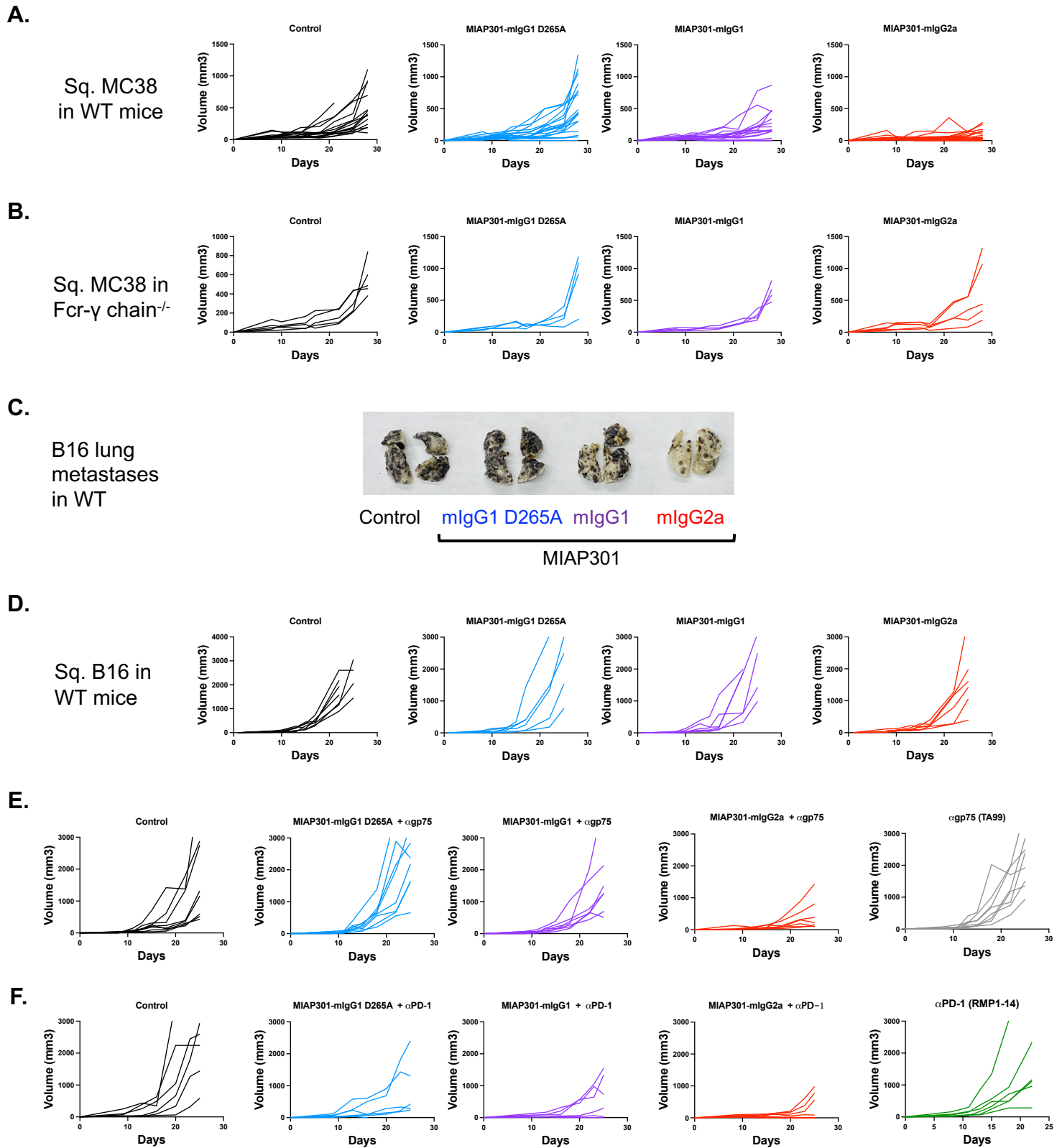
Zhao, X. W., Matlung, H. L., Kuijpers, T. W., and van den Berg, T. K. (2012b). On the mechanism of CD47 targeting in cancer. *Proc Natl Acad Sci U S A* *109*, E2843; author reply E2844-2845.

Supplementary Figure 1. Generation and validation of Fc variants for mouse and chimeric anti-CD47 antibodies



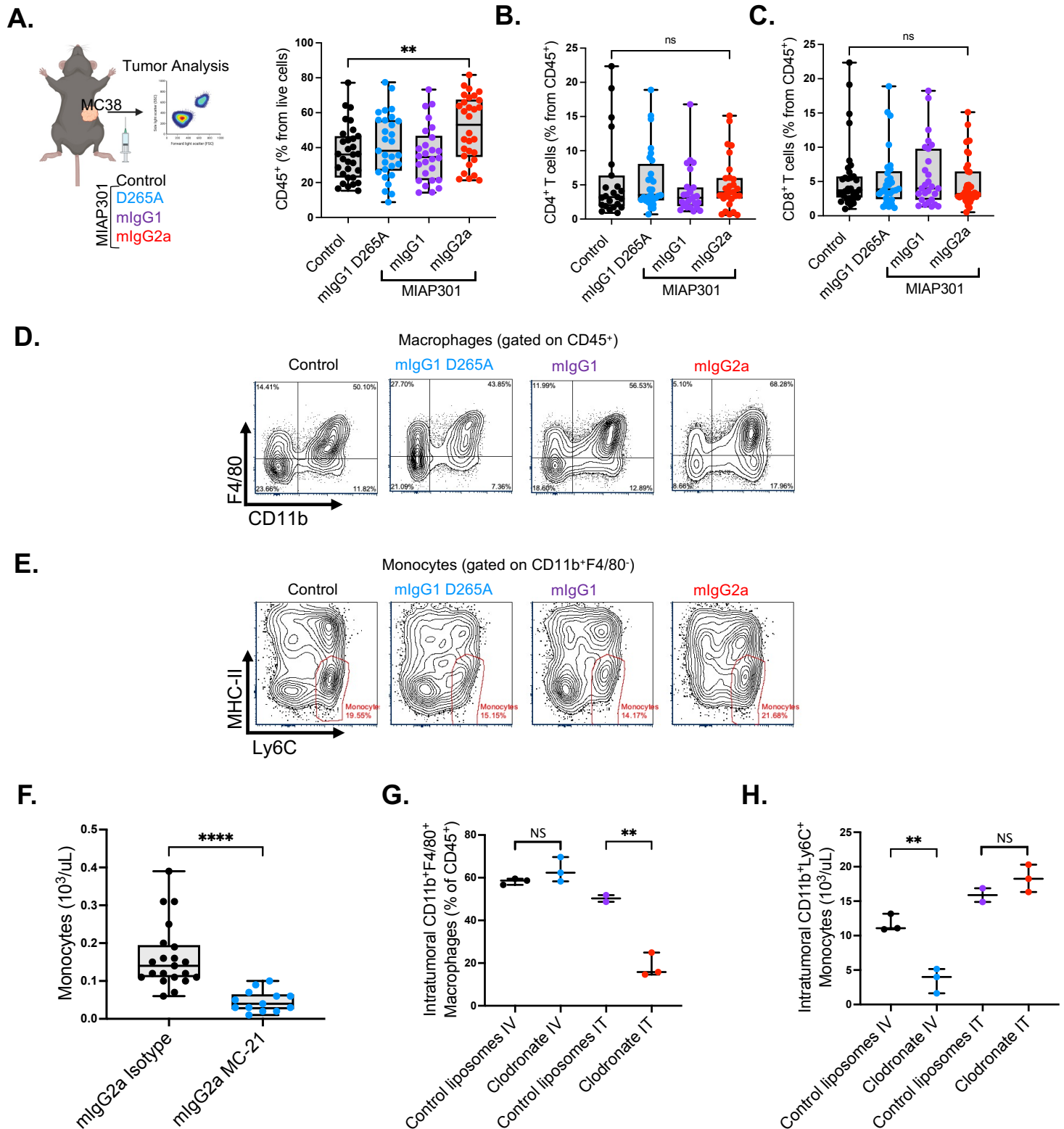
(A) Binding profiles to mouse FcγRs of Fc variants for anti-CD47 antibodies (MIAP301, chimeric-5F9 and chimeric-2D3), activating-to-inhibitory binding ratio (A/I) to mFcγRs is shown **(B)** Levels of expression of CD47 on different mouse cell lines, mean fluorescence intensity (MFI) expressed on the right. **(C)** Diagram showing the structure of the mouse antibody MIAP301 and binding of their Fc variants to recombinant mouse CD47 by ELISA **(D)** Diagram showing the structure of the chimeric antibody chimeric-5F9 and binding of their Fc variants to recombinant human CD47 by ELISA **(E)** Diagram showing the structure of non-blocking (Chimeric 2D3-mIgG2a) and blocking (Chimeric 5F9-mIgG2a) CD47 antibodies. Binding to recombinant human CD47 by ELISA **(F)** Competitive ELISA showing the capacity of blocking (mIgG2a Chimeric-5F9) and non-blocking (mIgG2a Chimeric-2D3) antibodies to disrupt the binding of recombinant SIRPα to hCD47.

Supplementary Figure 2. Engagement of activating Fc γ R_s enhances in vivo antitumor activity of MIAP301 ab



(A) Individual growth of sq. MC38 tumors in WT mice, **(B)** in mice lacking all activating Fc γ R_s (FcR- γ chain^{-/-}) that were treated with MIAP301 Fc variants or control (50 μ g IT, d. 8,10,14 and 18). **(C)** Representative images showing B16 lung metastases in WT mice after treatment with control or MIAP301 Fc variants (20 mg/Kg IP, d. 1,4,7 and 11). **(D)** Individual growth of sq. B16 tumors in WT mice, treated as monotherapy with MIAP301 Fc variants or control (50 μ g IT, d. 8,10,14 and 18); or **(E)** In combination with anti-gp75 ab (TA99-mIgG2a, 200 μ g IP d. 8, 10, 14 and 18); or **(F)** In combination with anti-PD-1 ab (RMP1-14-mIgG1-D265A, 200 μ g IP d. 8, 10, 14 and 18).

Supplementary Figure 3. Changes myeloid and T cells after treatment with Fc variants of anti-mCD47 ab and assessment of depletion of monocytes and macrophages.

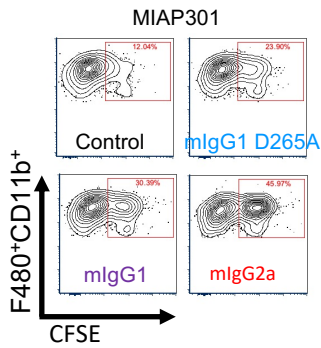


(A-C) Established MC38 tumors were analyzed by flow cytometry 72 hours after treatment with Fc variants for CD47 antibodies (MIAP301). Quantification of CD45⁺, CD4⁺ and CD8⁺ cells from MC38 tumors 72h after treatment with Fc variants is shown. (D) Representative flow cytometry plots of macrophages, and (E) monocytes 72h after treatment with MIAP301 Fc variants. (F) Peripheral blood levels of monocytes 24 hours after treatment with anti-CCR2 ab (Clone MC-21-mIgG2a, 100 ug) or isotype control in WT mice. (G) Quantification of intratumoral macrophages from MC38 tumors pre-treated with control- or clodronate-liposomes intravenously (IV) or intratumorally (IT) (100 uL, d.-3, -1) by flow cytometry. (H) Quantification of intratumoral monocytes from MC38 tumors pre-treated with control- or clodronate-liposomes intravenously (IV) or intratumorally (IT) (100 uL, d.-3, -1) by flow cytometry.

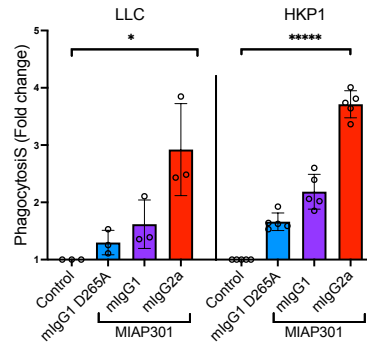
Supplementary Figure 4. Fc-enhanced anti-CD47 antibodies enhance in vitro antibody dependent cellular phagocytosis (ADCP) across different species-match systems

Effector cells: Macrophages from WT mice. Target: WT murine cancer cells. Tx: anti-mCD47 abs

A.

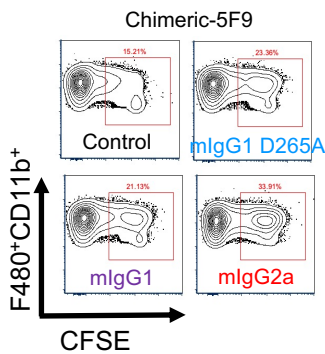


B.

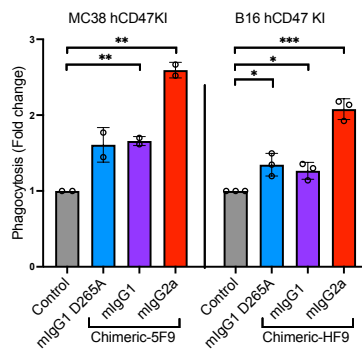


Effector cell: Macrophages from hCD47hSIRP α KI. Target: murine cancer cells hCD47KI. Tx: chimeric (mFc) anti-hCD47

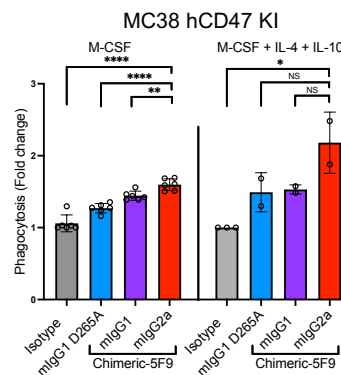
C.



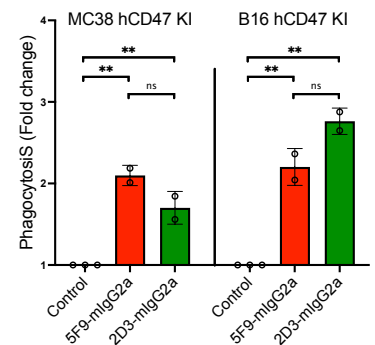
D.



E.

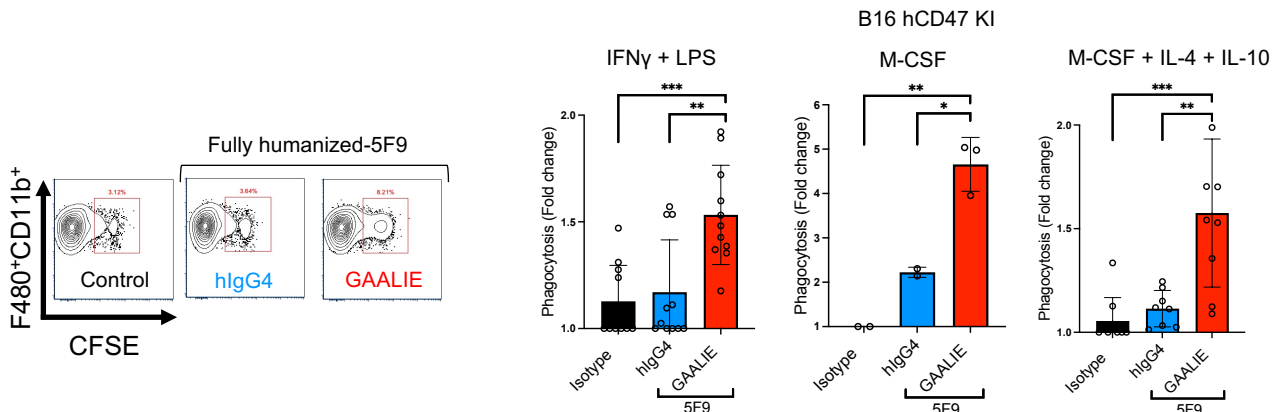


F.



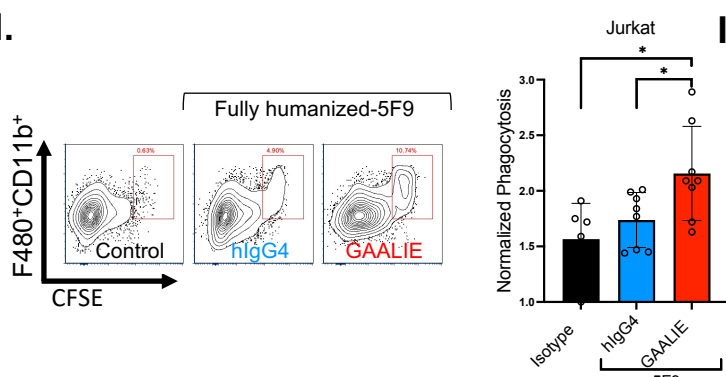
Effector cell: Macrophages from hCD47hSIRP/hFc γ R. Target: murine cancer cells hCD47KI. Tx: humanized (hFc) anti-hCD47

G.

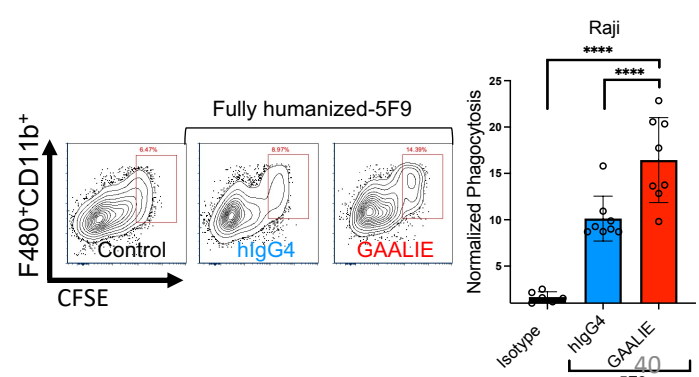


Effector cell: Macrophages from human PBMC. Target: human cancer cells. Tx: humanized (hFc) anti-hCD47

H.

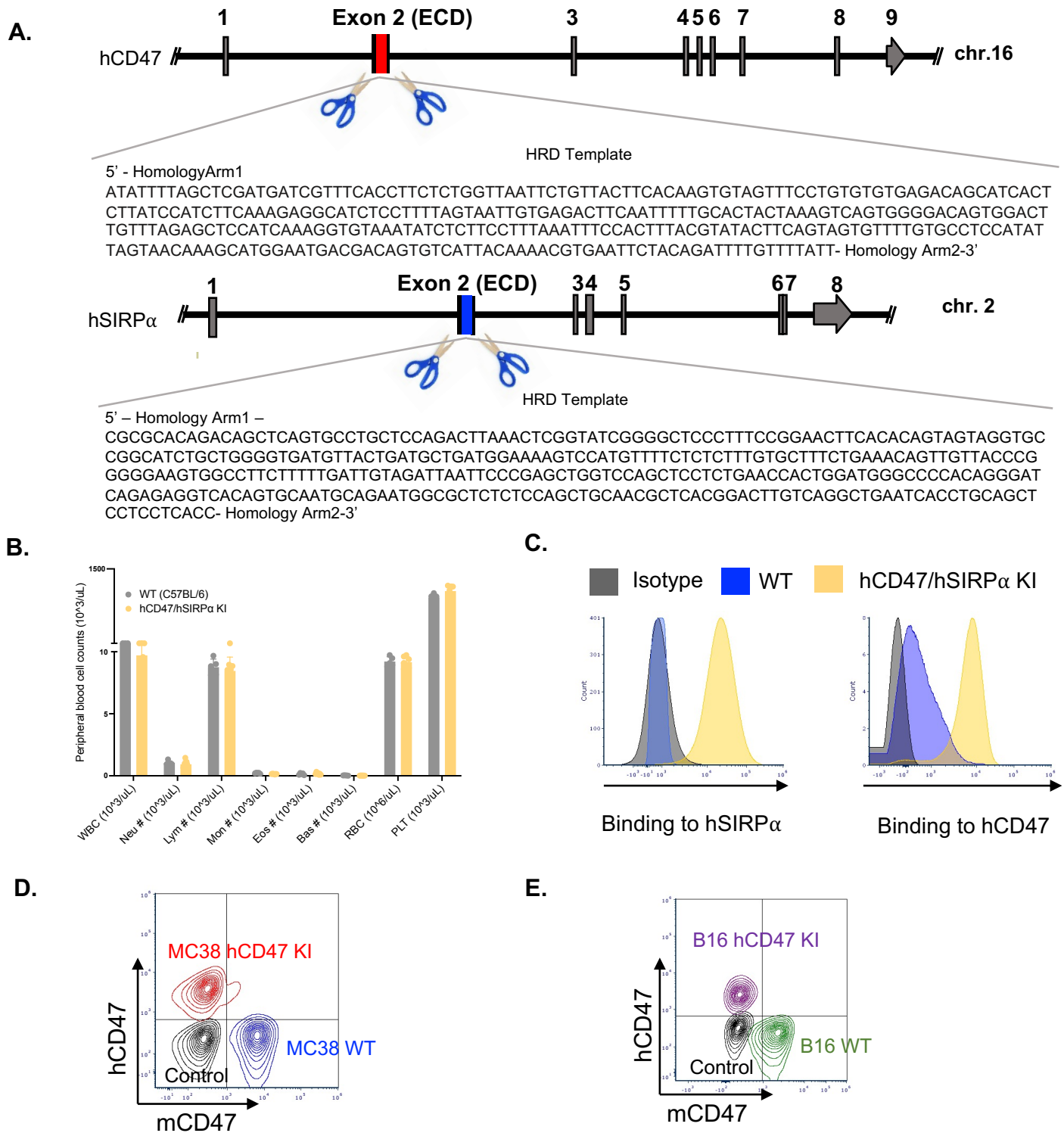


I.



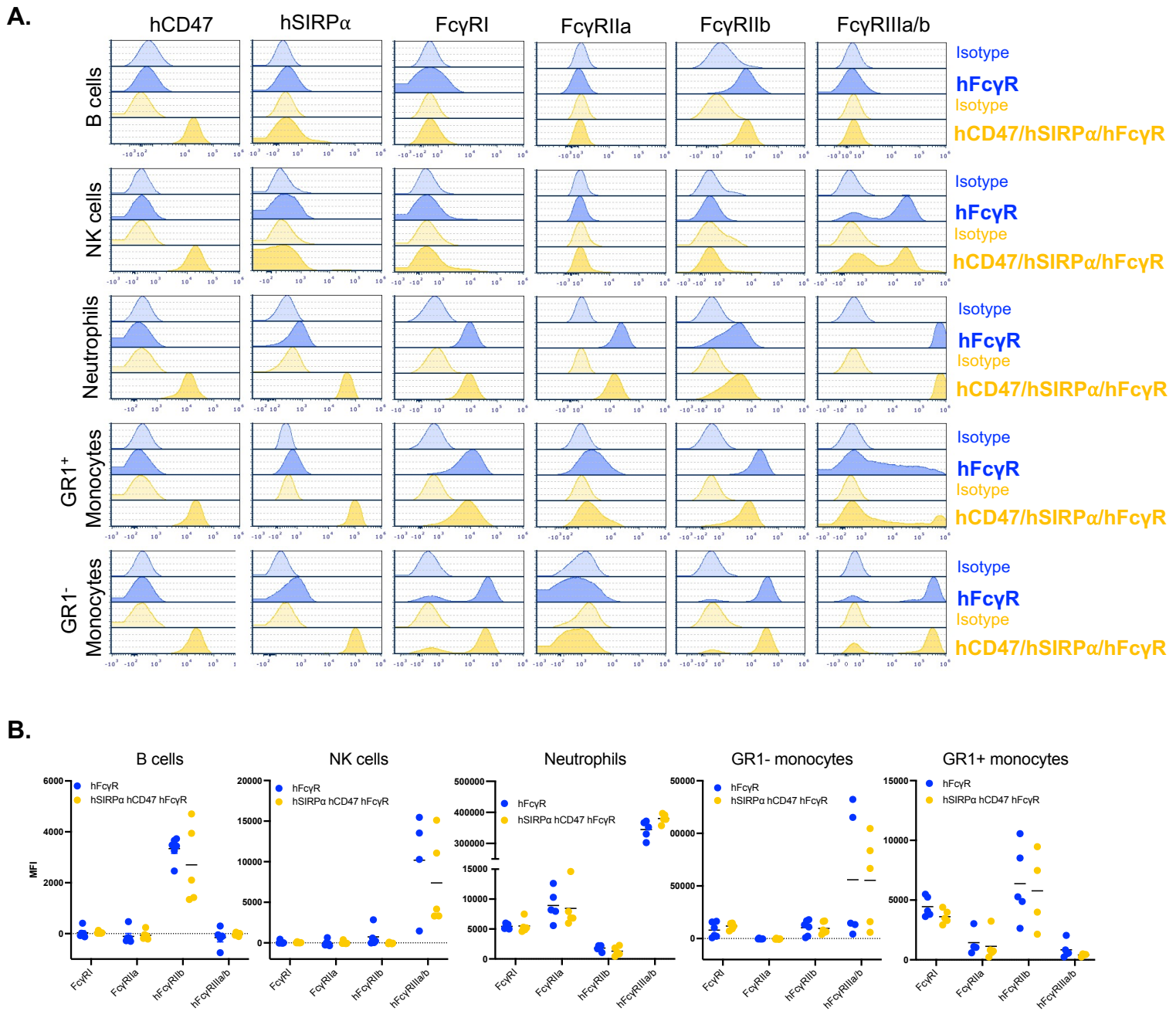
(A) Representative flow cytometry plots of the percentage of phagocytosis of B16 cancer cells by BMDM from WT mice after treatment with control or Fc subclasses of MIAP301. **(B)** Phagocytosis of Lewis lung carcinoma (LLC) or HKP1 (*Kras*^{G12D}*p53*^{-/-}) lung adenocarcinoma after treatment with control or Fc subclasses of MIAP301. **(C)** Representative flow cytometry plot and **(D)** phagocytosis of MC38 hCD47 KI or B16 hCD47 KI by BMDM from hCD47/hSIRP α KI mice after treatment with control or Fc variants of Chimeric-5F9. **(E)** Phagocytosis of MC38 hCD47 KI cells by BMDM from hCD47/hSIRP α KI mice pre-treated with different polarization conditions. **(F)** Phagocytosis of MC38 hCD47 KI or B16 hCD47 KI cells by BMDM from hCD47/hSIRP α KI mice after treatment isotype control, blocking (5F9), non-blocking (2D3) antibodies targeting hCD47, both in mIgG2a Fc format **(G)** (Left) Representative flow cytometry plots and (Right) phagocytosis of B16 hCD47 KI mice by BMDM from hCD47/hSIRP α /hFc γ R mice after treatment with Fc variants of fully humanized anti-CD47 ab (5F9). Macrophages were pre-treated with different polarization conditions as indicated. **(H)** (Left) representative flow cytometry plots and (right) phagocytosis of human cancer cell line Jurkat and **(I)** Raji by human macrophages derived from PBMCs after treatment with Fc variants of fully humanized 5F9.

Supplementary Figure 5. Development of humanized mouse model for CD47 and SIRP α (hCD47/hSIRP α KI mice) and cancer cell lines



(A) Schematic drawing showing CRISPR/Cas9-mediated gene-targeting strategy to generate CD47 (top) and SIRP α (bottom) KI mice. The double-strand break induced by the CRISPR/Cas9 in the flanking regions of the ECD of mCD47 and mSIRP α was replaced by their human counterparts via non-homologous end joining. **(B)** Complete cell blood count of WT and hCD47/hSIRP α KI mice **(C)** Right: Recombinant hSIRP α was incubated with RBCs from WT and hCD47/hSIRP α KI mice, binding was only detected in RBCs from the hCD47/hSIRP α mouse. Left: Recombinant hCD47 was incubated with leukocytes from WT and hCD47/hSIRP α KI mice, binding was primarily detected in leukocytes from the hCD47/hSIRP α mouse. **(D)** Flow cytometry analysis of expression of hCD47 and mCD47 in unstained (Black), MC38 WT (blue) and MC38 hCD47 KI cells (red). **(E)** Flow cytometry analysis of expression of hCD47 and mCD47 in unstained (Black), B16 WT (blue) and B16 hCD47 KI cells (red).

Supplementary Figure 6. Characterization of Fc γ R in mice humanized for CD47, SIRP α and Fc γ Rs



(A) Characterization of Fc γ R profile on mice humanized for Fc γ Rs (blue) and mice humanized for CD47, SIRP α and Fc γ Rs (yellow), representative flow cytometry plots and **(B)** Quantification are shown.